EXPOSURE TO NICKEL, CHROMIUM, OR CADMIUM CAUSES DISTINCT CHANGES IN THE GENE EXPRESSION PATTERNS OF RAT LIVER-DERIVED CELL LINES

by

Matthew G. Permenter

B.S. (The Pennsylvania State University) 1999

THESIS

Submitted in partial satisfaction of the requirements for the degree of

MASTER OF SCIENCE

in

ENVIRONMENTAL BIOLOGY

in the

GRADUATE SCHOOL

of

HOOD COLLEGE

May 2010

Accepted:

_____	_____
David Jackson, Ph.D.	April Boulton, Ph.D.
Thesis Advisor	Director, Environmental Biology Program
_____	_____
Drew Ferrier, Ph.D.	Allen P. Flora, Ph.D.
Committee Member	Dean of the Graduate School
_____	
Oney Smith, Ph.D.	
Committee Member	

REPORT DOCUMENTATION PAGE

Form Approved
OMB No. 0704-0188

PLEASE DO NOT RETURN YOUR FORM TO THE ABOVE ADDRESS.

1. REPORT DATE *(DD-MM-YYYY)*	2. REPORT TYPE	3. DATES COVERED *(From - To)*
22-May-2010	Master's Thesis	August 2008 - May 2010

4. TITLE AND SUBTITLE

Exposure to Nickel, Chromium, or Cadmium Causes Distinct Changes in the Gene Expression Patterns of Rat Liver-Derived Cell Lines

5a. CONTRACT NUMBER

5b. GRANT NUMBER

5c. PROGRAM ELEMENT NUMBER

PE 622787

6. AUTHOR(S)

Matthew G. Permenter

5d. PROJECT NUMBER

.D2

5e. TASK NUMBER

3.N

5f. WORK UNIT NUMBER

7. PERFORMING ORGANIZATION NAME(S) AND ADDRESS(ES)

U.S. Army Center for Environmental Health Research
568 Doughten Drive
Fort Detrick, MD 21702-5010

8. PERFORMING ORGANIZATION REPORT NUMBER

9. SPONSORING/MONITORING AGENCY NAME(S) AND ADDRESS(ES)

U.S. Army Medical Research and Materiel Command
504 Scott Street
Fort Detrick, MD 21702-5012

10. SPONSOR/MONITOR'S ACRONYM(S)

USAMRMC

11. SPONSOR/MONITOR'S REPORT NUMBER(S)

12. DISTRIBUTION/AVAILABILITY STATEMENT

Approved for Public Release; Unlimited Distribution.

13. SUPPLEMENTARY NOTES

14. ABSTRACT

Nickel, cadmium, and chromium are toxic industrial chemicals with an exposure risk, found in military, occupational, and environmental settings. While the substances are known to have adverse health effects, the exact mechanisms of toxicity remain unclear and a paucity of biomarkers of exposure and effect exist. To identify candidate biomarkers and to elucidate the mechanisms of toxicity of Ni, Cr, and Cd, H4-II-E-C3 and MH1C1 rat liver-derived cell lines were treated with various concentrations of each metal and gene expression patterns were determined through the use of an Affymetrix microarray and analzyed using bioinformatic tools including Ingenuity Pathway Analysis. A total of 992 probe sets were differentially expressed as a result of exposure to nickel, chromium, and/or cadmium, 246 of which may be further investigated as candidate biomarkers. The modulated genes were involved in biological processes such as the oxidative stress response, apoptosis, cell cycle regulation, and hypoxia.

15. SUBJECT TERMS

nickel, cadmium, chromium, biomarkers, microarray, heavy metals, liver

16. SECURITY CLASSIFICATION OF:			17. LIMITATION OF ABSTRACT	18. NUMBER OF PAGES	19a. NAME OF RESPONSIBLE PERSON
a. REPORT	b. ABSTRACT	c. THIS PAGE			Carol O'Brien
U	U	U	SAR	101	19b. TELEPHONE NUMBER *(Include area code)* 301-619-7685

Reset

Standard Form 298 (Rev. 8/98)
Prescribed by ANSI Std. Z39.18

INSTRUCTIONS FOR COMPLETING SF 298

1. REPORT DATE. Full publication date, including day, month, if available. Must cite at least the year and be Year 2000 compliant, e.g. 30-06-1998; xx-06-1998; xx-xx-1998.

2. REPORT TYPE. State the type of report, such as final, technical, interim, memorandum, master's thesis, progress, quarterly, research, special, group study, etc.

3. DATES COVERED. Indicate the time during which the work was performed and the report was written, e.g., Jun 1997 - Jun 1998; 1-10 Jun 1996; May - Nov 1998; Nov 1998.

4. TITLE. Enter title and subtitle with volume number and part number, if applicable. On classified documents, enter the title classification in parentheses.

5a. CONTRACT NUMBER. Enter all contract numbers as they appear in the report, e.g. F33615-86-C-5169.

5b. GRANT NUMBER. Enter all grant numbers as they appear in the report, e.g. AFOSR-82-1234.

5c. PROGRAM ELEMENT NUMBER. Enter all program element numbers as they appear in the report, e.g. 61101A.

5d. PROJECT NUMBER. Enter all project numbers as they appear in the report, e.g. 1F665702D1257; ILIR.

5e. TASK NUMBER. Enter all task numbers as they appear in the report, e.g. 05; RF0330201; T4112.

5f. WORK UNIT NUMBER. Enter all work unit numbers as they appear in the report, e.g. 001; AFAPL30480105.

6. AUTHOR(S). Enter name(s) of person(s) responsible for writing the report, performing the research, or credited with the content of the report. The form of entry is the last name, first name, middle initial, and additional qualifiers separated by commas, e.g. Smith, Richard, J, Jr.

7. PERFORMING ORGANIZATION NAME(S) AND ADDRESS(ES). Self-explanatory.

8. PERFORMING ORGANIZATION REPORT NUMBER. Enter all unique alphanumeric report numbers assigned by the performing organization, e.g. BRL-1234; AFWL-TR-85-4017-Vol-21-PT-2.

9. SPONSORING/MONITORING AGENCY NAME(S) AND ADDRESS(ES). Enter the name and address of the organization(s) financially responsible for and monitoring the work.

10. SPONSOR/MONITOR'S ACRONYM(S). Enter, if available, e.g. BRL, ARDEC, NADC.

11. SPONSOR/MONITOR'S REPORT NUMBER(S). Enter report number as assigned by the sponsoring/ monitoring agency, if available, e.g. BRL-TR-829; -215.

12. DISTRIBUTION/AVAILABILITY STATEMENT. Use agency-mandated availability statements to indicate the public availability or distribution limitations of the report. If additional limitations/ restrictions or special markings are indicated, follow agency authorization procedures, e.g. RD/FRD, PROPIN, ITAR, etc. Include copyright information.

13. SUPPLEMENTARY NOTES. Enter information not included elsewhere such as: prepared in cooperation with; translation of; report supersedes; old edition number, etc.

14. ABSTRACT. A brief (approximately 200 words) factual summary of the most significant information.

15. SUBJECT TERMS. Key words or phrases identifying major concepts in the report.

16. SECURITY CLASSIFICATION. Enter security classification in accordance with security classification regulations, e.g. U, C, S, etc. If this form contains classified information, stamp classification level on the top and bottom of this page.

17. LIMITATION OF ABSTRACT. This block must be completed to assign a distribution limitation to the abstract. Enter UU (Unclassified Unlimited) or SAR (Same as Report). An entry in this block is necessary if the abstract is to be limited.

COPYRIGHT WAIVER

I authorize Hood College to lend this thesis, or reproductions of it, in total or in part, at the request of other institutions or individuals for the purpose of scholarly research.

DEDICATION

I would like to dedicate this thesis to my wife, Amy. Without her this journey never would have begun, and without her support, never would have been completed.

ACKNOWLEDGMENTS AND SPONSORSHIP

The research conducted in this thesis would not have been possible without the generous support of The United States Army Center for Environmental Research, Dr. John Lewis, COL Matthew Schofield, LTC Andrea Stahl, and Martin Nau and Dr. Maryanne Vahey at the Walter Reed Army Institute of Research Vaccine Genomics Laboratory.

TABLE OF CONTENTS

TABLE OF CONTENTS (CONTINUED)

LIST OF TABLES

LIST OF FIGURES

ABSTRACT

Nickel, cadmium, and chromium are toxic industrial chemicals with an exposure risk, found in military, occupational, and environmental settings. While the substances are known to have adverse health effects, the exact mechanisms of toxicity remain unclear and a paucity of biomarkers of exposure and effect exist. To identify candidate biomarkers and to elucidate the mechanisms of toxicity of Ni, Cr, and Cd, H4-II-E-C3 and MH1C1 rat liver-derived cell lines were treated with various concentrations of each metal and gene expression patterns were determined through the use of an Affymetrix microarray and analyzed using bioinformatic tools including Ingenuity Pathway Analysis. A total of 992 probe sets were differentially expressed as a result of exposure to nickel, chromium, and/or cadmium, 246 of which may be further investigated as candidate biomarkers. The modulated genes were involved in biological processes such as the oxidative stress response, apoptosis, cell cycle regulation, and hypoxia.

INTRODUCTION

In the line of duty American soldiers are not only in danger from hostile action, but also from the environment surrounding them. One such risk to the warfighter, as well as to the general public, is the exposure to Toxic Industrial Chemicals (TICs) and Toxic Industrial Materials (TIMs). Diagnosis and treatment of an exposure is often difficult as these substances can have an irregular distribution in the environment and individuals may respond differently to them. They are deemed as large of a threat as chemical warfare agents since they are readily available, produced in large amounts, and may similarly degrade mission performance (McKone et al. 2000).

Recently, soldiers in the field have been exposed to TICs and TIMs that were both deliberately spread and encountered in the environment as a pollutant. In 2003, National Guard troops in Iraq were exposed to hexavalent chromium while protecting contractors who were repairing the Qarmat Ali Water Treatment Plant in Basrah, Iraq (The Associated Press 2009). The burn pit at Joint Base Balad has also received considerable recent media attention when soldiers reported illnesses they attributed to inhaling toxic smoke emanating from the burn pit (U.S. Army Center for Health Promotion and Preventive Medicine 2008).

The general public is also at risk of exposure to TICs and TIMs in the environment or as a result of occupational hazards. From 1980 to 1983 a national survey conducted by the National Institute for Occupational Safety and Health estimated that 727,240 workers were potentially exposed to nickel metal, nickel alloys, or nickel compounds (ATSDR 2005a). Additionally, approximately 9,000 hazardous substance

releases were reported to occur annually in the 15 states taking part in the CDC Hazardous Substances Emergency Events Surveillance system (ATSDR 2005b).

The heavy metals nickel (Ni), cadmium (Cd), and chromium (Cr) are examples of TICs that have a military, occupational, and environmental relevance. Nickel is used in producing batteries and stainless steel, creating an occupational and environmental hazard as discussed above. It has also been considered by the military for use as an alloy with tungsten and cobalt as an environmentally friendly replacement for depleted uranium munitions, but was dismissed when the alloy was shown to be extremely carcinogenic (Kalinich et al. 2005). Chromium is often used as a pigment or as an anti-corrosive, making it a potential pollutant to the environment or soldiers, such as in the case at the Qarmat Ali water treatment plant (Barceloux 1999). Cadmium is frequently encountered as an occupational hazard since it is commonly used in pigments, batteries, and welding, a ubiquitous practice in both the military and industry (Meo and Al-Khlaiwi 2003).

While Ni, Cd, and Cr are widely used and have been well characterized, few biomarkers currently exist and their exact mechanisms of toxicity remain unclear. All three chemicals are thought to cause oxidative stress, which is capable of inducing DNA damage and protein degradation (Beyersmann and Hartwig 2008). Nickel and chromium undergo Fenton type reactions forming reactive oxygen species, while cadmium is thought to cause oxidative stress through the inhibition of antioxidant enzymes (Beyersmann and Hartwig 2008, Stohs et al. 2001). Chromium is the only metal of the three that is able to directly interact with DNA, forming Cr-DNA adducts and causing

DNA damage, while nickel and cadmium are thought to cause DNA damage through the inhibition of repair enzymes (Beyersmann and Hartwig 2008). Nickel is the only metal of the three that has been shown to mimic hypoxia, up-regulating genes involved in many cellular processes such as glycolysis and apoptosis through the stabilization of the transcription factor HIF-1α (Salnikow et al. 2004). Ni, Cd, and Cr are also thought to cause deregulation of cell proliferation through various signaling pathways and transcription factors, perhaps due to reactive oxygen species (ROS), although the activation of these pathways is poorly understood (Beyersmann and Hartwig 2008).

An individual's exposure to these toxic chemicals is often difficult to detect and treat since responses and clinical signs to these substances vary greatly; however biomarkers may serve as diagnostic tools to identify an exposure. The FDA defines biomarkers as characteristics that are objectively measured and evaluated as indicators of normal biologic processes, pathogenic processes, or pharmacologic responses to a therapeutic intervention (U.S.Department of Health and Human Services, Food and Drug Administration, Center for Drug Evaluation and Research, & Center for Biologics Evaluation and Research 2008). A chemical or its metabolite in a person's body fluid may serve as a biomarker, or it may be a gene expression change that results from an exposure to a substance. A biomarker may not necessarily be a single characteristic, but may be a group of them forming a signature or fingerprint of response. Unfortunately, few biomarkers of effect, such as enzymes, intermediates, or breakdown products, have been identified and validated for use in humans due to the previous lack of appropriate analytical methods and computational power. Biomarker discovery is a difficult process

due to the lengthy path from candidate discovery to clinical assay and the lack of a rigorous and comprehensive process for biomarker development (Dalmasso 2008).

The advancing field of toxicogenomics has a range of new technologies, such as microarray technology, data analysis, and bioinformatic processes and tools, which may aid in the discovery of new biomarkers. Toxicogenomics evaluates changes in gene expression in response to environmental agents or toxicants, allowing for genome-wide assessment of gene expression changes resulting from such exposures. DNA microarrays measure the abundance of thousands of gene transcripts simultaneously, providing a snapshot of what is occurring inside a cell at a given moment. Statistical and normalization methods have been developed to handle differences between samples and the large amounts of data generated by a microarray experiment. Perhaps the greatest challenge of microarray technology is assigning biological meaning to the large amount of data generated. Many different bioinformatic programs, applications, and methods have been developed to aid in deciphering microarray results, including programs to cluster similarly behaving genes and to provide insight into function and pathway analysis. Therefore, toxicogenomics provides tools to analyze gene expression changes that can provide possible targets for genomic biomarkers as well as understanding the mechanisms of toxicity.

In order to identify candidate biomarkers and to elucidate the mechanisms of toxicity of Ni, Cr (VI), and Cd, toxicogenomic and bioinformatic methods were used to investigate gene expression patterns of rat liver based *in vitro* systems. H4-II-E-C3 (H4IIE) cells were selected as they are well characterized and metabolically active liver

models (Michels et al. 2006). MH1C1 cells, another well characterized and liver-like cell line (Odashima et al. 1979), were then used to confirm the results were reflective of hepatocyte-like function. MH1C1 and H4-II-E-C3 (H4IIE) cells were exposed to nickel (II) chloride ($NiCl_2$), cadmium chloride ($CdCl_2$), and sodium dichromate ($Na_2Cr_2O_7$). Affymetrix microarrays were used to evaluate the quantity of specific mRNA sequences present in the samples. Statistical software tools were used to determine whether significant changes occurred with treatment to the various toxicants. Bioinformatics software and applications were applied to decipher the biological meaning of the gene expression patterns to aid in determining the mechanisms of toxicity and identifying candidate biomarkers. Differentially expressed genes involved in the known mechanisms for the three metals, such as apoptosis, cell cycle control, DNA damage, and hypoxic response were identified.

MATERIALS AND METHODS

Cell Culture Conditions and Exposures

MH1C1 and H4IIE cells (ATCC, Manassas, VA) were grown to near confluency in Dulbecco's Modified Eagle's Medium (DMEM) (Lonza,Walkersville, MD) with 10% fetal bovine serum (FBS) (Invitrogen, Carlsbad, CA) and 10 mL Glutamax (Invitrogen) at 37 ºC and 5% carbon dioxide in T75 flasks. Exposures were initiated once flasks were 90 +/- 10% confluent using the test chemicals $NiCl_2 \cdot 6H_2O$, $CdCl_2$, and $Na_2Cr_2O_7$ (Sigma-Aldrich, St. Louis, MO). Exposure doses were chosen at the no observable effect level, 20% effect, and 50% effect based on the CellTiter-Fluor Cell Viability and CellTiter 96 Aqueous Non-Radioactive Cell Proliferation Assays (Promega, Madison, WI) for each cell line (Table 1). Each flask was washed twice with serum free DMEM to remove residual serum components, as the media will be used in a parallel proteomic study, with a 5 minute incubation between washes. Fifteen mL of serum free DMEM containing the proper concentration of toxicant was added to each flask for 24 hours. Four biological replicates were performed for each condition, including a control containing only DMEM with 10% FBS and 10 mL Glutamax. The medium with the toxicant was removed from each flask and flash frozen for use in future projects after the 24 hours exposure period.

RNA Extraction

The cells were manually scraped from the surface of the flask and homogenized using a Dounce homogenizer (Dounce and Lan 1943). Total RNA was extracted using Trizol solution per the manufacturer’s instructions for RNA Isolation (Invitrogen). An

Table 1: Exposure concentrations (in µM) for the (a.) H4IIE and (b.) MH1C1 cell lines.

a.

Dose	Nickel	Chromium	Cadmium
Low	40	0.275	0.20
Mid	140	1.000	0.55
High	400	10.000	1.20

b.

Dose	Nickel	Chromium	Cadmium
Low	30	15	2
Mid	300	180	4
High	1800	400	8

RNeasy Midi Kit cleanup (Qiagen, Germantown, MD) was performed as per the manufacturer's instructions to remove residual salts and organic solvents. RNA quality and quantity was determined through the use of the Agilent Bioanalyzer Series II RNA 6000 Nano LabChip Kit (Palo Alto, CA).

Microarray Preparation and Processing

cDNA and labeled cRNA was prepared per Affymetrix's GeneChip Expression Analysis Technical Manual using 7.5 µg total RNA. Twenty micrograms of biotin-labeled cRNA was sent to the laboratory of Dr. Maryanne Vahey at the Walter Reed Army Institute of Research Vaccine Genomics Laboratory for fragmentation, hybridization, staining, washing, and scanning on the GeneChip Rat Genome 230 2.0 Array according to the manufacturer's instructions (Affymetrix, Santa Clara, CA).

Data Normalization and Statistical Analysis

Microarray data was processed for background adjustment, normalization, and summarization using the Robust Multi-Array Averaging method (RMA) (Irizarry et al. 2003) using Partek software, version 6.4 Copyright 2009 (St. Louis, MO). The microarray data was visually examined for outliers using Principal Component Analysis (PCA) in Partek Pro, a method of reducing the multi-dimensional data sets to lower dimensions that can be readily visualized. Samples were compared using pairwise correlation analysis and replicate versus replicate dot plots of all probe sets in Microsoft Excel (Bellevue, WA) to verify inter-replicate reproducibility. Replicates were accepted with a R^2>0.95 and no gross deviations from linearity. If a sample did not meet these

criteria, a new microarray was processed from the total RNA. A present, absent, or marginal detection call for each probe set was determined by the Affymetrix GCOS algorithm and only probe sets with a present detection call for all samples in at least one condition were retained for analysis (Archer and Reese 2010).

The probe sets that met the present detection criteria underwent a 3-way ANOVA with the variables chemical, dose, and "batch" between each chemical treatment condition and the control using Partek. The batch variable was included to control for differences observed in the PCA resulting from different experimental and processing dates (Figure 1). Statistical significance was determined by the Benjamini and Hochberg False Discovery Rate (FDR) (Benjamini and Hochberg 1995) and a fold change filter was applied. Probe sets with a FDR less than or equal to 0.001 and a 1.8 or greater fold change from control in at least one treatment condition were retained for bioinformatic analysis.

qPCR Validation

Quantitative Polymerase Chain Reaction (qPCR) was used to validate the microarray results from the toxicant exposures to the H4IIE cell line. The total RNA from the four biological replicates of the toxicant exposures used for microarray analysis were also used for qPCR validation with the genes and primers (Integrated DNA Technologies, Skokie, IL) shown in Table 2. The primers were designed using Primer Express software (Applied Biosystems, Foster City, CA) based on the Reference Sequence mRNA (Pruitt et al. 2007). cDNA was prepared from total RNA using the Advantage RT-for-PCR kit per the manufacturer's instructions published April 2006 (Clonetech, Mountain View,

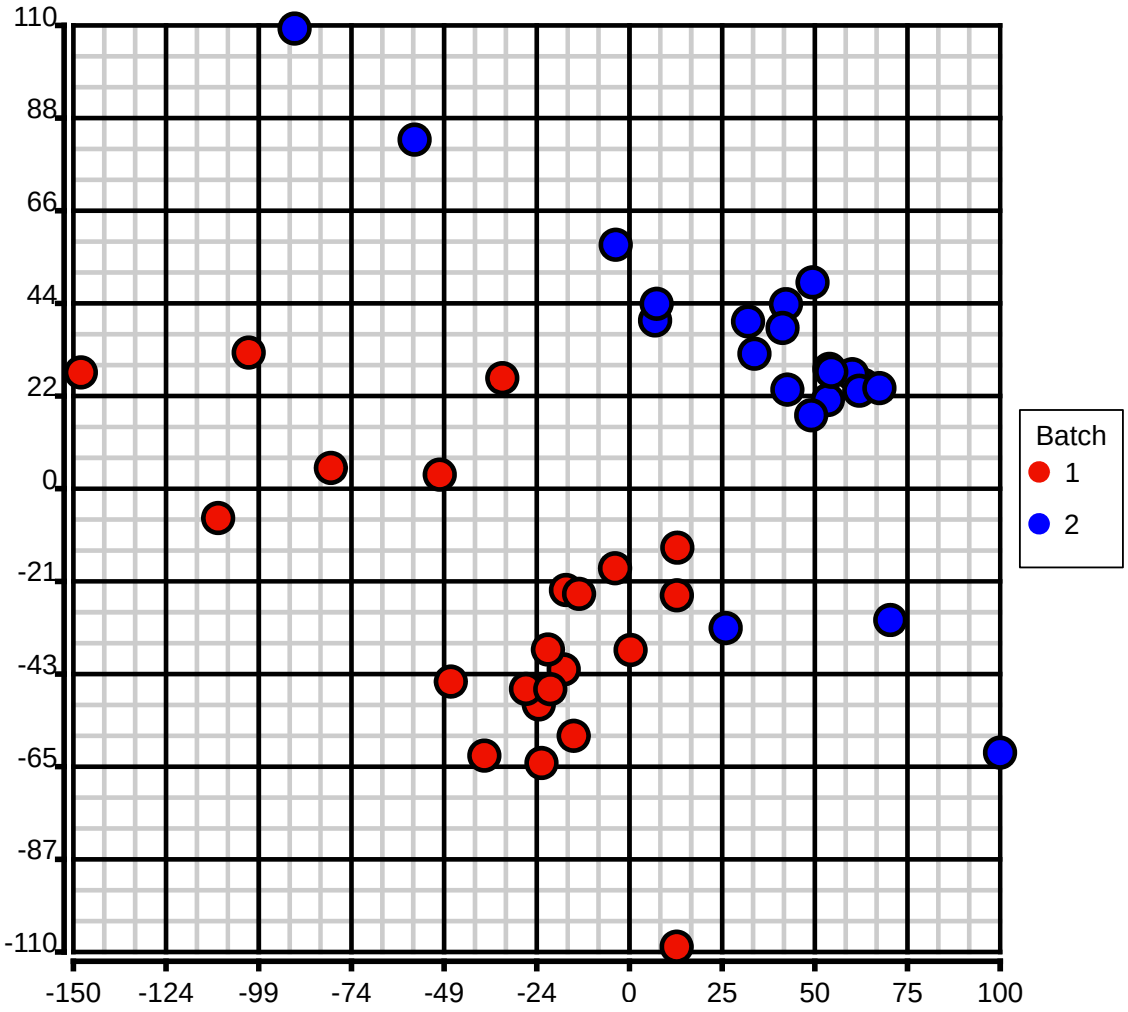

Figure 1: Principal component analysis (PCA) of probe sets present in all four replicates of at least one treatment condition in H4IIE cells. PCA is a data reduction tool used to visualize the variability in an experiment. In this case, each data point represents one microarray. This plot illustrates a batch effect as the microarrays form two distinct groups based on the dates of the experiments.

Table 2: Genes and Primers used for qPCR validation

Gene	Role in Cell	Forward Primer	Reverse Primer
Actb	Regulation of actin cytoskeleton	CTGTGTGGATTGGTGGCTCTATC	AGAAAGGGTGTAAAACGCAGCT
Gapdh	Glycolysis	GGATACTGAGAGCAAGAGAGAGGC	GATGGTATTCGAGAGAAGGGAGG
Adm	Oxidative stress response	CTAGCGAGGAAAAGTGCAATGC	TCGCTTTAAAATGCCCTTAATACA
Atf	Stress response, cell cycle control	CACAACATTGGCGTGATTTTTT	CTCGGTCAGCACAGAGTAGCAC
Cdt	DNA replication	TTAAGCTTCCCTGTCTGCATCA	TCCAGAGTCTACGTCCCCTATAGC
Fabp1	Oxidative stress response	CTATGGGTCCAAGGTGATCCAC	AATTCAGTCACGGACTTTATGCCT
Gadd45	DNA repair, cell cycle arrest	GCAGAGCTGTTGCTACTGGAGAA	TTCCCGGCAAAAACAAATAAGT
Slc39a10	Metal ion transporter	CTACACCGGTACCATAGCTGCTT	ACGTCTTACACGTCACTGCACC

CA). The Applied Biosystems SYBR Green Master Mix was used in a 50 µl qPCR reaction with 2 µl of cDNA template and a 2.5 µM final concentration of each primer for a total of 8 genes, 2 of which served as the endogenous controls. A DNA Opticon 2 (Bio-Rad, Hercules, CA) was used for thermal cycling and fluorescence detection using the following scheme: 95 °C for 10 minutes followed by 40 cycles of: 95 °C for 15 seconds, 60 °C for 1 minute, and a fluorescence signal read. Relative fold change was determined using the comparative C_t method (Livak and Schmittgen 2001) and values from the four biological replicates were averaged. The microarray results were compared to the qPCR results using Pearson's product-moment correlation coefficient.

Bioinformatics

Multiple exploratory software packages were used for bioinformatic analysis of statistically significant changing genes identified in the H4IIE cell line. The probe sets determined to be modulated by toxicant exposure and their expression values were imported into VxInsight using VxArrayImport 0.2.5 with default settings (Sandia National Laboratories, Albuquerque, NM) for cluster analysis (Kim et al. 2001). Clusters were manually selected by their natural boundaries using the terrain view, and probe sets in each cluster were exported to Excel for further use.

Ingenuity Pathways Analysis (Ingenuity Systems, www.ingenuity.com, analysis date 2009-11-09) was used to explore the biological implications of the data. Core analysis were performed on the data using the Rat Genome 230 2.0 Array as the reference set with all other default settings selected. Networks, canonical pathways, and biological

functions that were statistically significant, as determined by the software, were examined.

Gene Ontology Tree Machine (Zhang et al. 2004) was also used as a data exploration tool. The probe sets from each VxInsight cluster were imported into the program with *Rattus norvegicus* selected as the species and "rnorvegicas_affy_rat230_2" selected as the gene ID type. All probe sets that had a present detection call in all four replicates of at least one treatment condition were uploaded for a reference set with "rnorvegicas_affy_rat230_2" selected as the gene ID type. The hypergeometric method was used to determine statistical significance with a Benjamini and Hochberg multiple test adjustment. A significance level of 0.05 was used, and a minimum of 2 genes present in a category was required to test the significance of that category. The Directed Acyclic Graph (DAG) was examined for statistically significant enriched gene ontology (GO) terms.

IPA and Gene Ontology Tree Machine (GOTM) only identified biological functions of a small subset of the differentially expressed genes; therefore, a manual "binning" method was devised. This scheme identified the major biological processes that were modulated by treatment with the toxicants by assigning probe sets to groups, or bins, based on GO categories. Seven bin categories were created based on known effects of nickel, chromium, and cadmium in the published literature: cell cycle, oxidative stress, ion homeostasis, apoptosis, energy regulation, hypoxic response, and DNA damage, replication, and repair. Each bin was compromised of multiple, related GO terms based on the GO biological process terms provided by Affymetrix in the annotation file

for the Rat Genome 230 2.0 Array (build 29, 2009-7-13). The GO terms found in each bin can be found in Appendix 1. Probe sets were then assigned to a bin if the GO term associated with that probe set was also contained in that particular bin. A chi-squared test was used to determine statistical significance of enriched bins for each VxInsight cluster. Expected values for each bin in the chi-squared test were calculated by the ratio of probe sets in a bin to the total number of probe sets in a data set containing all probe sets with present detection calls in all replicates of one treatment condition that contained at least one biological process GO term in the Affymetrix annotation file. Probe sets that did not contain any biological process annotation were not considered for significance testing.

RESULTS

Data Normalization and Statistical Analysis

The .cel file of the microarray data was RMA preprocessed and outliers were identified using a PCA plot, multivariate correlation, and replicate vs. replicate dot plots. Probe sets that were not detected above the background level were removed from the analysis, leaving 16,311 out of the 31,099 possible probe sets for further analysis. A three way ANOVA (chemical, dose, and batch) was run, the FDR computed, and the fold change was calculated for each treatment compared to the control. A probe set with an FDR equal to or less than 0.001 and a fold change of at least 1.8 was considered to be differentially expressed. The analysis identified 430 probe sets in the nickel, 456 probe sets in the chromium, and 288 probe sets in the cadmium treatment groups as modulated. Since many of the probe sets were statistically significant in more than one chemical, a total of 992 probe sets overall were identified as differentially expressed (Figure 2 and Appendix 2-8). Hierarchical clustering of differentially expressed genes using Euclidean distance for row dissimilarity produced a heat map providing a visualization of the probe sets' expression patterns across all treatment conditions (Figure 3). The hierarchical clustering showed that some probe sets were responding to only a single metal while others were responding to two or three, and that response occurred in a dose dependant manner.

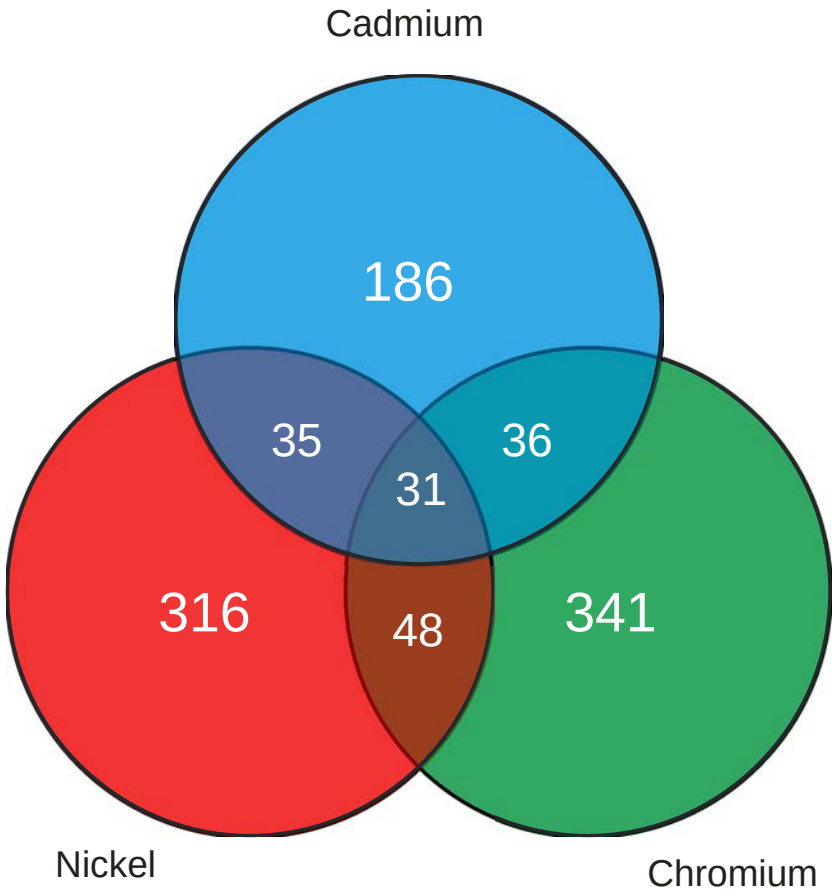

Figure 2: Venn diagram showing the distribution of the 992 differentially expressed (FDR<0.001 and 1.8 fold change) probe sets in the H4IIE cell line among the exposures to nickel, chromium, or cadmium.

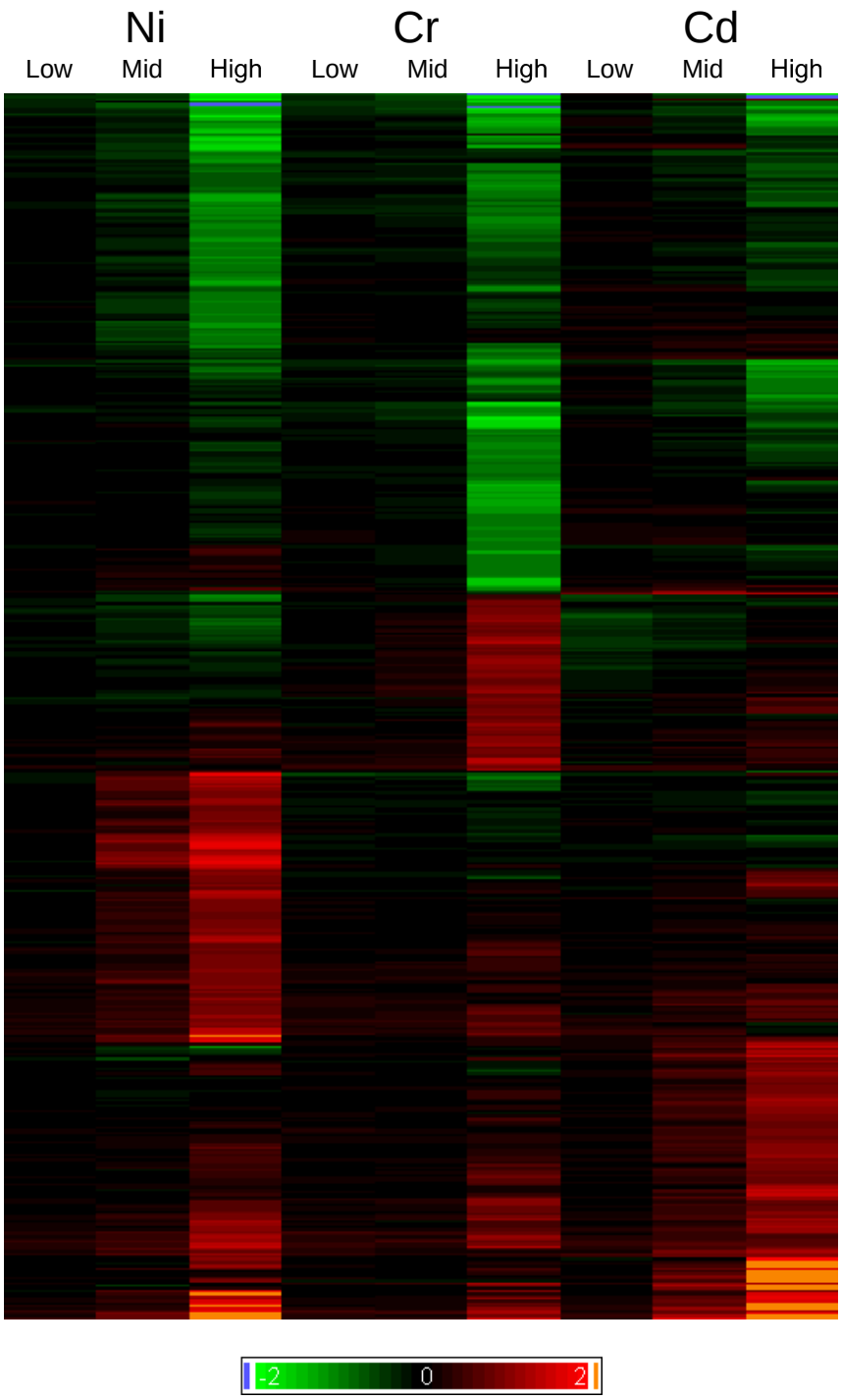

Figure 3: Hierarchical clustering of 992 differentially expressed probe sets showing some were responding to only a single metal while others were responding to two or all three, and that the response did display a dose dependence. Each column represents a treatment condition and each row represents the $\log_2$ ratio of change from the control sample of an individual probe set.

qPCR Validation

Validation of the microarray results was conducted by qPCR analysis. Six genes that were differentially expressed by nickel, chromium, and/or cadmium were chosen for validation. Care was taken to choose genes that were over expressed or repressed by each of the three chemicals. Overall, a successful validation was considered to be at least a 1.8-fold change in the same direction in the qPCR and microarray experiments.

The comparative C_t method was used to determine fold change differences using *Actb* and *Gapdh* mRNA as endogenous controls. The qPCR results of the six genes used for validation, *Gadd45*, *Slc39a10*, *Cdt*, *Atf*, *Fabp1*, and *Adm* successfully validated the microarray results, as all were changing by at least two fold in the same direction (Figure 4). Pearson's correlation was also calculated between the qPCR and microarray results. The fold change of all genes between the qPCR and microarray results were highly correlated with r values for *Gadd45*, *Fabp1*, *Slc39a10*, *Cdt*, *Atf*, and *Adm* of 0.95, 0.92, 0.96, 0.99, 0.91 and 0.97 respectively.

Cluster and Pathway Analysis of Microarray Data

The 992 probe sets were imported into VxInsight to identify similarly behaving and presumptively co-regulated probe sets through cluster analysis (Kim et al. 2001). The cluster analysis groups together genes with similar regulation or function which can be explored using pathway analysis tools. VxInsight uses a force directed placement algorithm to move similar items closer together while simultaneously pushing dissimilar objects away from each other and then displays the relationships on a 3D terrain-like map

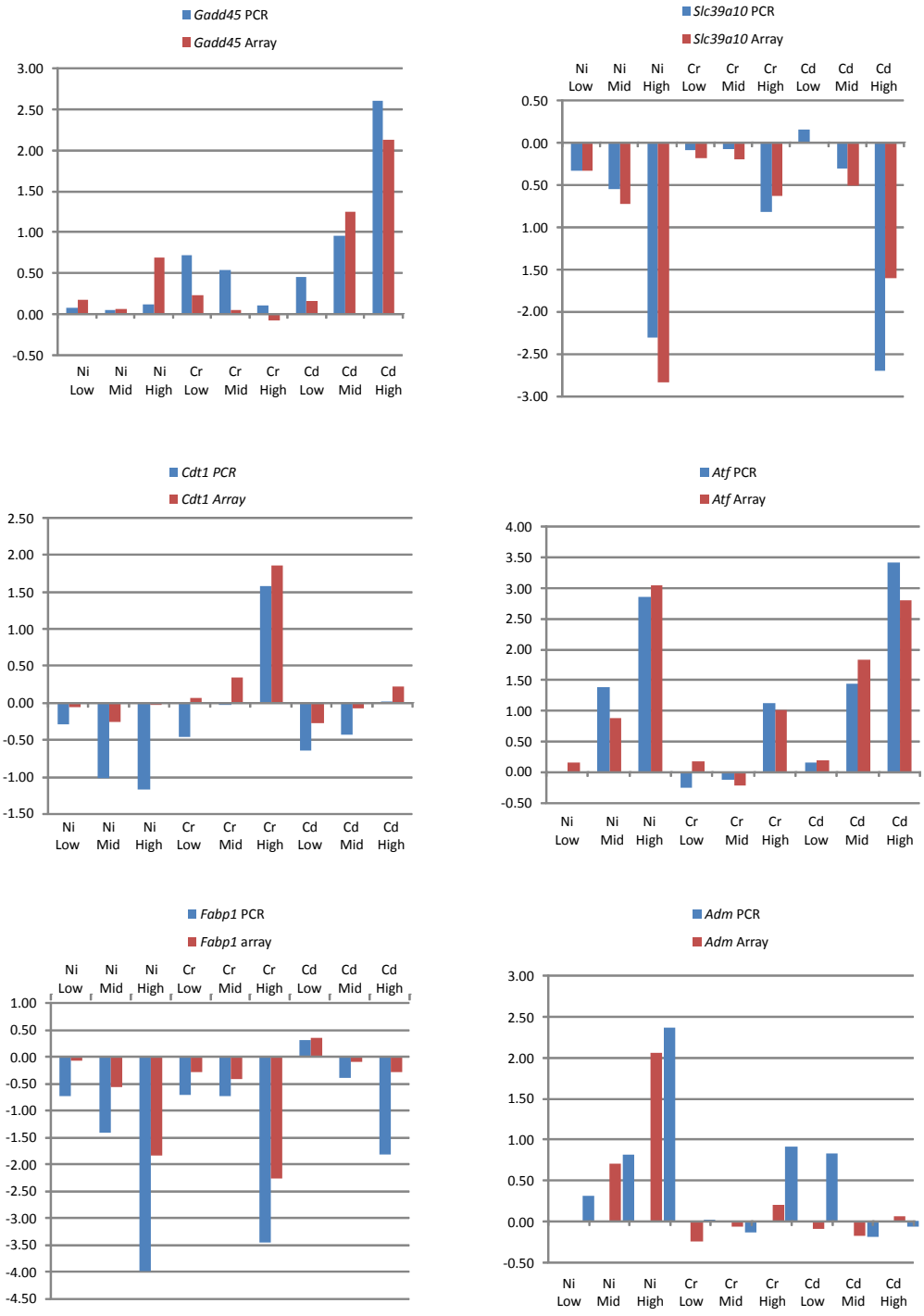

Figure 4: Gene expression changes detected by qPCR and microarray are highly correlated. The results are displayed as $\log_2$ ratio of change from control.

(Boyack et al. 2002). Four clusters were identified and the probe sets of each were highlighted in either blue, white, yellow, or green (Figure 5 and Appendix 2). Each of the four clusters represents a different subset of probe sets that were differentially expressed in the three metals (Figure 6). The blue cluster was mainly comprised of probe sets that were up-regulated in nickel while the white cluster contained probe sets that were mostly up-regulated in chromium only. The probe sets in the green cluster were up-regulated in just about every metal, but most heavily in cadmium. The yellow cluster generally contains probe sets that are down regulated in all three chemicals.

The probe sets contained in each VxInsight cluster were imported into Ingenuity Pathway Analysis (IPA) for canonical pathway analysis to identify known pathways affected by treatment to the toxicants (see Figure 7 for a complete list). A canonical pathway in IPA is a well characterized metabolic or cell signaling pathway that was drawn based on the IPA Knowledge Base. The only canonical pathway that was significantly enriched ($p \leq 0.05$) in more than one cluster was the NRF2-mediated oxidative stress response. The HIF1α signaling and glycolysis/gluconeogenesis pathways were also enriched in the blue cluster. VDR/RXR activation and ATM, and p53 signaling were all significantly enriched in the green cluster. In the white cluster only the pyrimidine metabolism and purine metabolism canonical pathways were enriched. Twenty-two different canonical pathways were enriched in the yellow cluster, most of which were involved in metabolism, the complement system, or acute phase response.

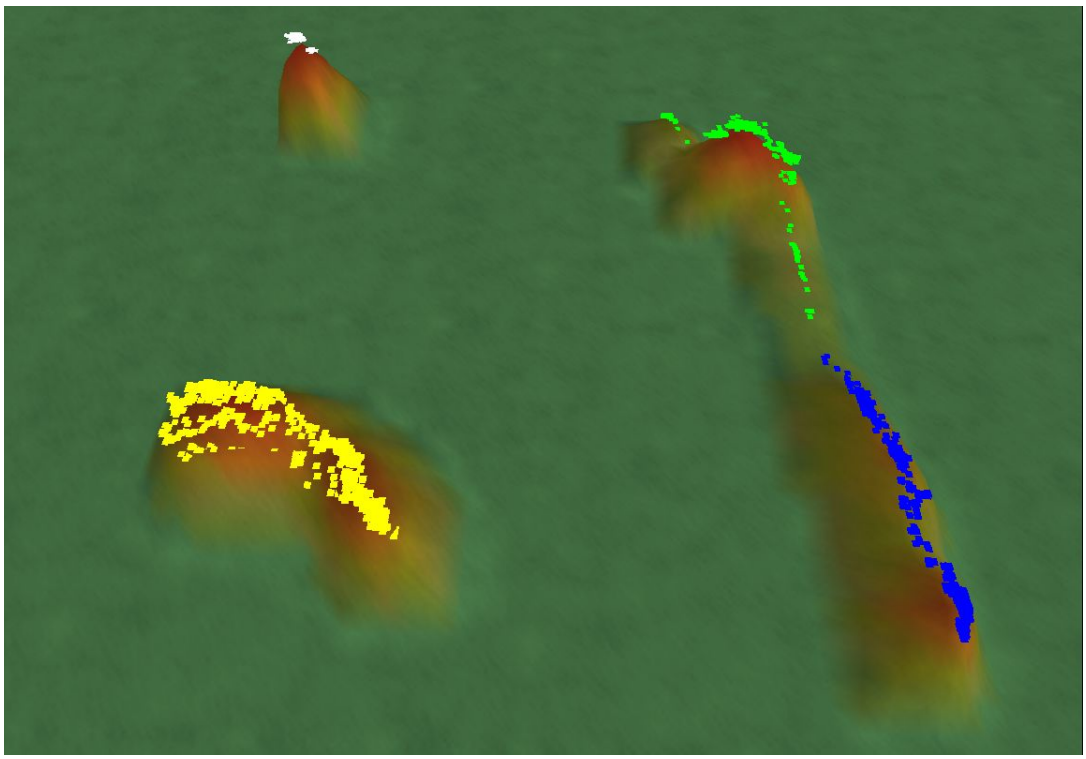

Figure 5: Cluster analysis of 992 differentially expressed probe sets using VxInsight, which clusters together probe sets with similar expression patterns. Each colored point represents one probe set, and the height of each peak is proportional to the number of data points beneath it. Probe sets with similar expression patterns cluster closely together while those that are different are further apart. Four distinct clusters were identified; the white, blue, green, and yellow clusters.

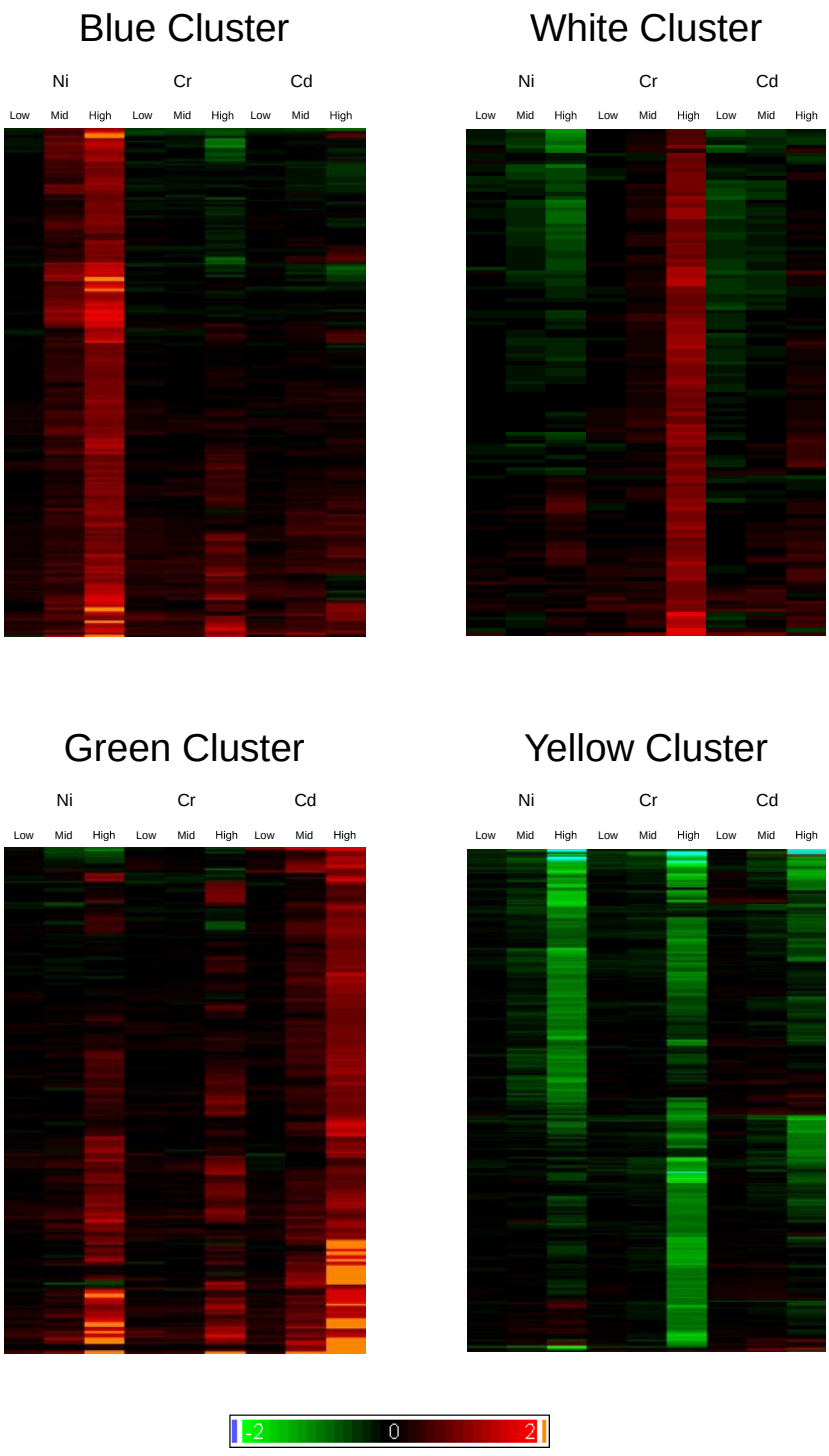

Figure 6: Hierarchical clustering of differentially expressed probes sets representing the blue, white, green, and yellow clusters generated by VxInsight are presented. The white, blue, and green clusters are comprised of probe sets up-regulated to Cr, Ni, and Cd respectively, while the green cluster contains genes down-regulated in response to all three metals. Gene expression values are provided as $\log_2$ ratio of change.

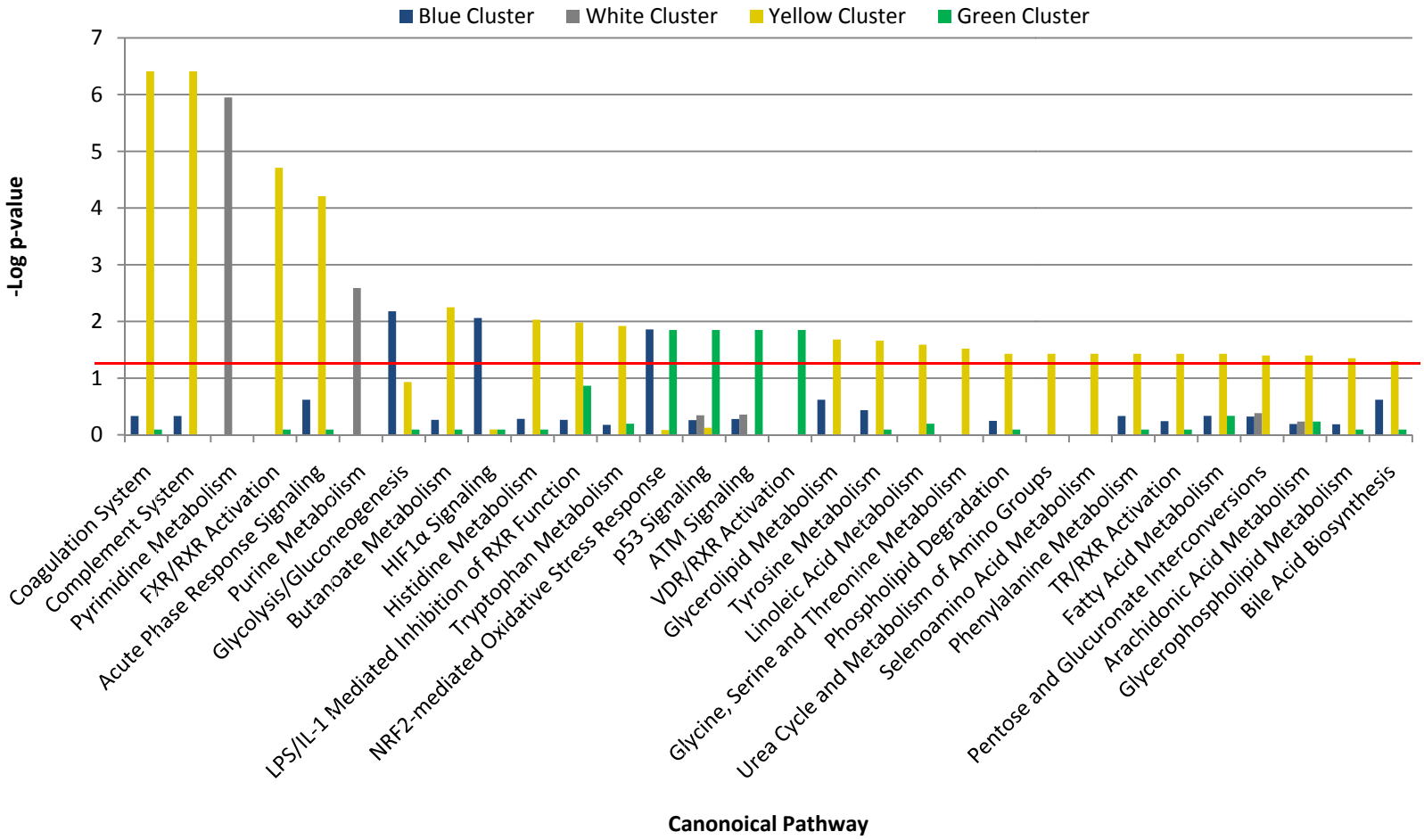

Figure 7: The graph displays the negative log of Benjamini and Hochberg false discovery rates of IPA canonical pathways based on VxInsight clusters showing pathways enriched by the probe sets contained in each cluster. The red line represents a 0.05 significance level cutoff.

The bio functions of the four VxInsight clusters were also determined using IPA to further elucidate mechanism of toxicity (see Figure 8 for a complete list). IPA bio functions associate biological functions and complex interactions from the Ingenuity Knowledge Base with the experimental data set. Many of the functions involved in such processes as cellular growth and cell death are significantly enriched ($p \leq 0.05$) in all clusters. Five functions, cellular development, cell cycle, cellular movement, DNA replication, recombination, and repair, and cellular compromise, are all enriched in the blue, white, and green cluster. These data suggest that all three chemicals are interfering with the cell cycle and causing DNA damage since the blue, white, and green clusters contain the majority of up-regulated probe sets across all chemical treatments.

To determine standardized gene ontology terms that were enriched, a process not possible using IPA, the probe sets in each VxInsight cluster were imported into Gene Ontology Tree Machine (GOTM). Statistical significance was determined using the hypergeometric test with a Benjamini and Hochberg False Discovery Rate multi test correction. GO categories were deemed to be significantly enriched at or below an adjusted p-value of 0.05. The third level gene ontology categories are listed in Table 3. Using higher level gene ontology provides little information, while a lower level provides too much detail to list, but is useful as an exploratory tool.

IPA and GOTM only provided function annotation for a small amount of probe sets identified as differently expressed; therefore, the probe sets in each VxInsight cluster for which Affymetrix annotation was available were assigned to a bin based on matching GO terms (Figure 9). The seven bins were based on known effects of the metals available

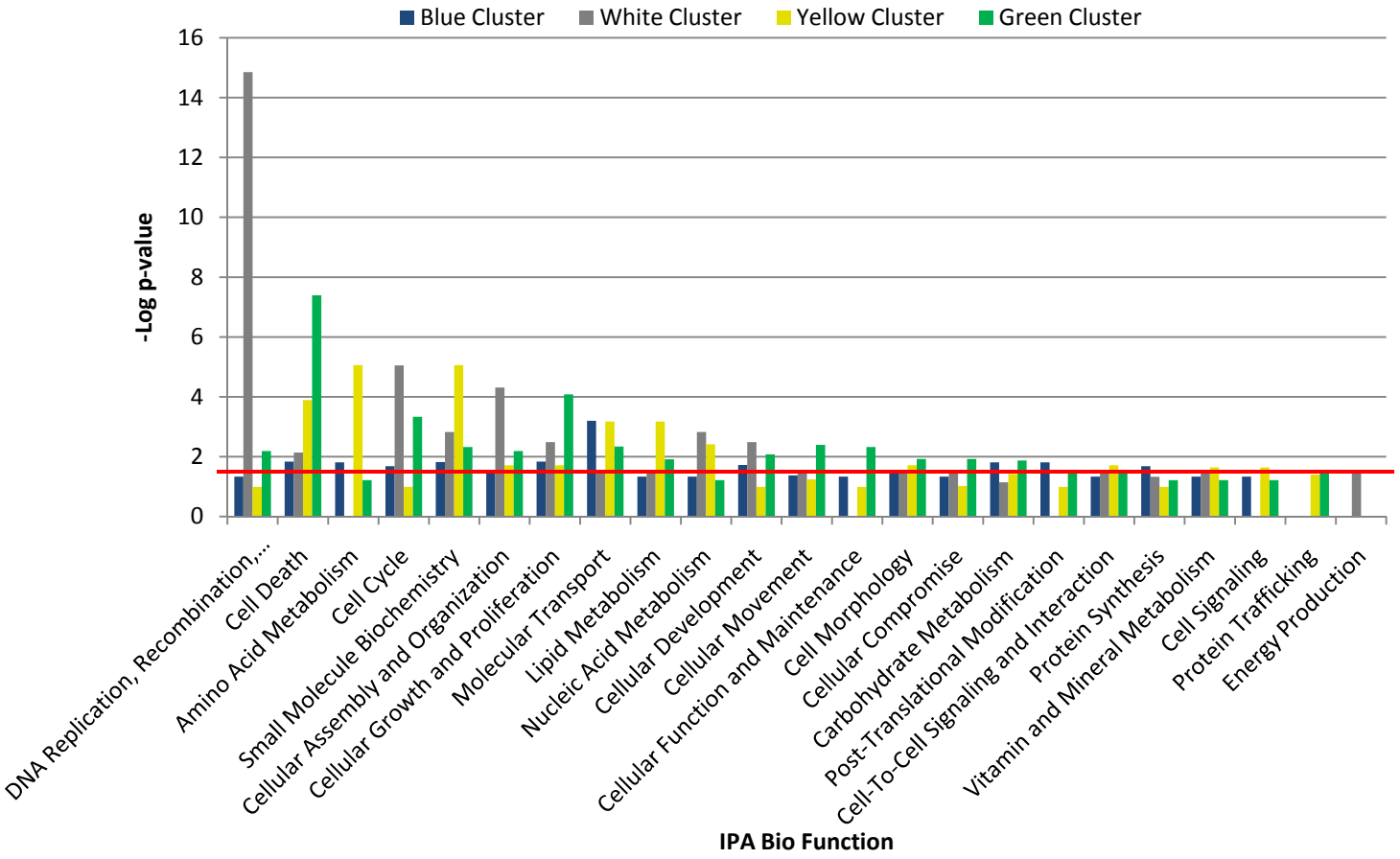

Figure 8: The graph displays the negative log of Benjamini and Hochberg false discovery rates of IPA bio function enrichment based on VxInsight clusters. The red line represents a 0.05 significance level cutoff.

Table 3: Significant third level biological process and molecular functions of VxInsight clusters as determined through the use of Gene Ontology Tree Machine (GOTM). The third level is being displayed as it presents a usable amount data without being too general.

Cluster	Biological Process	Molecular Function
Blue	Circulatory System Process Homeostatic Process Response to Oxygen Levels Response to Nitrosative Stress	L-ascorbic Acid Binding Cation Binding Identical Protein Binding Protein Dimerization Activity Dioxygenase Activity Oxidoreductase Activity Acting on Single and Paired Donors with Incorporation of Molecular Oxygen
White	Biosynthetic Process Nitrogen Compound Metabolic Process Macromolecule Metabolic Process Cellular Response to Stimulus	DNA Binding Purine Nucleoside Binding Hydrolase Activating Ligase Activity Forming Nitrogen-Metal Bonds
Green	Negative Regulation of Molecular Function Cell Death Regulation of Anatomical Structure Size Negative Regulation of Biological Processes System Development	None
Yellow	Extracellular Structure Organization Coagulation Digestion Organic Ether Metabolic Process Oxidation Reduction Catabolic Process Regulation of Hormone Levels	Phospholipid Binding Steroid Binding Polysaccharide Binding Sugar Binding Ligase Activity forming Carbon-Sulfur Bonds Carbon-Nitrogen Lyase Activity Monooxygenase Activity Transferase Activity Transferring Nitrogenous Groups Peptidase Activity Peptidase Inhibitor Activity Lipid Transporter Activity Heme Transport Activity

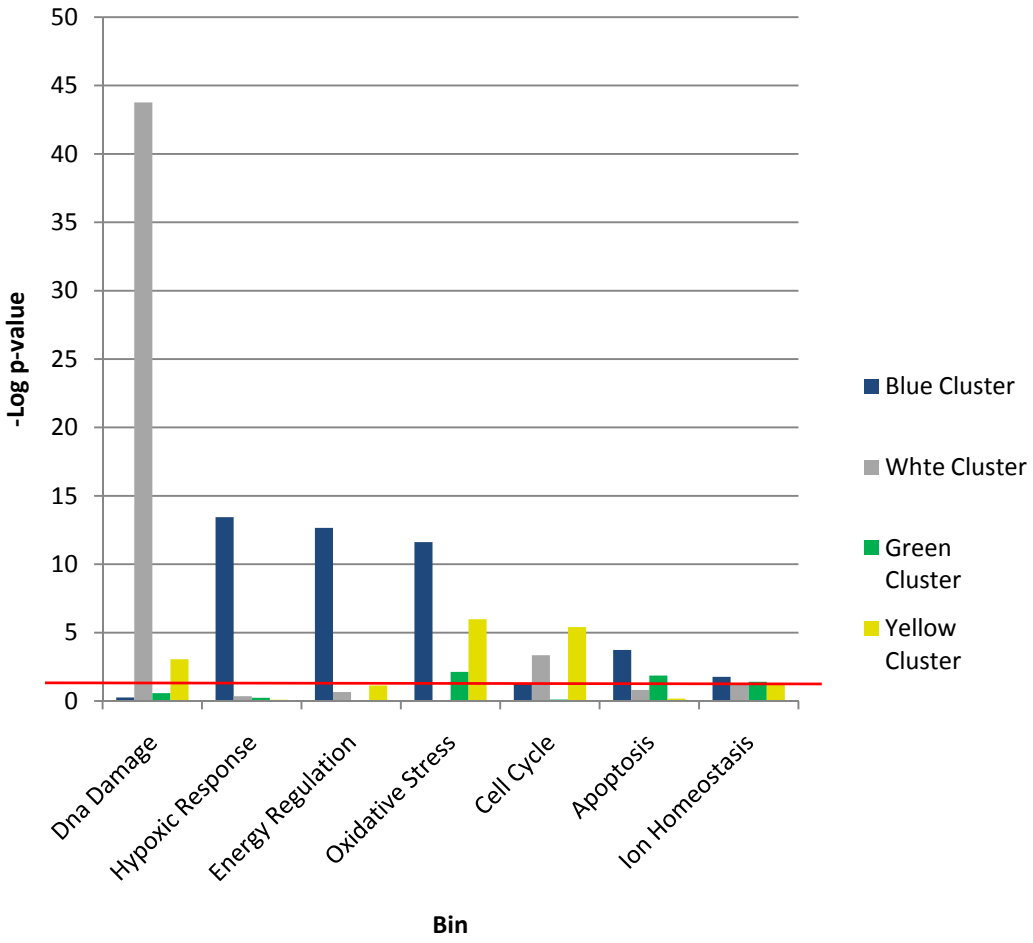

Figure 9: The graph displays the bin enrichment significance (-log p-value) by VxInsight cluster. The red line represents a 0.05 significance level cutoff. The bin method supported the mechanisms of toxicity suggested by the other bioinformatic applications.

in the current literature and were termed cell cycle, oxidative stress, ion homeostasis, apoptosis, energy regulation, hypoxic response, and DNA damage, replication, and repair. Statistical significance of bin enrichment was determined using a chi squared test with a p-value of 0.05 or less considered significant. In the blue cluster, the oxidative stress, ion homeostasis, apoptosis, energy regulation, and hypoxic response bins were all significantly enriched. In the white cluster, DNA damage, replication, and repair and cell cycle were the only bins significantly enriched. Oxidative stress, ion homeostasis, and apoptosis were all significantly enriched in the green cluster. The yellow cluster resulted in an enrichment of the DNA damage, replication and repair, oxidative stress, and cell cycle bins.

Bin enrichment was also investigated based on the individual chemicals to determine if any of the bin categories were affected solely by nickel, chromium, or cadmium exposure (Figure 10). A chi-squared test between a bin and the expected value was performed to determine statistical significance, with a p-value of 0.05 or less considered significant. The DNA damage, oxidative stress, cell cycle, energy regulation, and hypoxic response bins were all enriched in the probe sets modulated due to nickel exposure. The probe sets with differential expression due to chromium treatment resulted in the DNA damage, replication, and repair and oxidative stress bins being significantly enriched. The oxidative stress, ion homeostasis, apoptosis, and energy regulation bins were enriched by the probe sets modulated by treatment with cadmium. The bins significantly enriched are consistent with the known effects of the three chemicals such as the induction ROS causing oxidative stress resulting in apoptosis and disruption of the cell cycle.

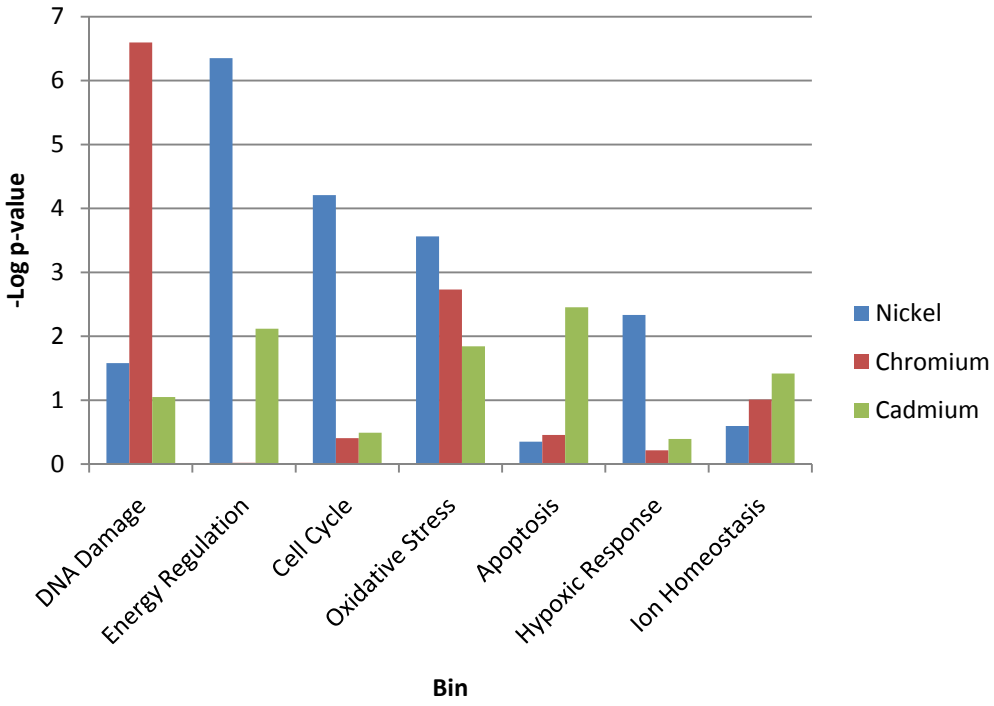

Figure 10: The graph shows the bin enrichment significance by metal as the negative log of the p-value. The data supports the mechanisms of toxicity of the metals suggested by the other bioinformatic methods as well as those identified in the literature.

Candidate Biomarker Identification

All differentially expressed probe sets in the H4IIE cell line were initially considered genes of interest for further study as biomarkers. Of the 992 differentially expressed probe sets identified in the H4IIE cell line, 812 were also differentially expressed in the MH1C1 cell line. Only probe sets that were associated to a gene by the Affymetrix annotation file were retained, as this ensures that only genes with known function are being considered. Those genes not changing by 2.5 fold in one treatment condition were also discarded, as smaller changes may be too small to serve as indicators of exposure. The remaining genes were then compared against the differentially expressed genes of the MH1C1 cell line. This comparison provided an opportunity to validate and test the differentially expressed genes identified as genes of interest in another rat liver-derived cell line. If the gene was not changing by 1.8 fold in the MH1C1 cells due to treatment to the same chemical it was discarded from consideration as a candidate biomarker. Genes that were not behaving similarly in both cell lines, or that had conflicting results from different probe sets for the same gene, were also removed. This resulted in 9 genes being identified as candidate biomarkers for all 3 chemicals, 39 for Cd, 99 for Cr, six for both Cr and Cd, 63 for Ni, 19 for Ni and Cd, and 11 for Ni and Cr (Table 4).

Table 4: Candidate biomarker genes in the chemicals of interest.

Gene	Chemical	Gene	Chemical	Gene	Chemical
Aldob	Ni, Cd, Cr	ProCr	Cd	Ezh2	Cr
Atf3	Ni, Cd, Cr	Ptrh1	Cd	F5	Cr
C5	Ni, Cd, Cr	RGD1560812	Cd	Fbxo5	Cr
Ddc	Ni, Cd, Cr	RGD1561551	Cd	Fen1	Cr
Hmox1	Ni, Cd, Cr	S100a11	Cd	Gamt	Cr
Itih4	Ni, Cd, Cr	Slc3a2	Cd	Gca	Cr
Klf5	Ni, Cd, Cr	Slc41a2	Cd	Ghr	Cr
Maff	Ni, Cd, Cr	Tnfrsf12a	Cd	Gins3	Cr
Zfand2a	Ni, Cd, Cr	Tnfrsf21	Cd	Hal	Cr
Abcc2	Cd	Trib3	Cd	Hnrnpa1	Cr
Abhd2	Cd	Trim16	Cd	Igsf11	Cr
Abhd3	Cd	Trim26	Cd	Inadl	Cr
Axud1	Cd	Wars	Cd	Iqub	Cr
Bag3	Cd	Abca8	Cr	Itpr1	Cr
Ces2	Cd	Adk	Cr	Kif16b	Cr
Cnn3	Cd	Apob	Cr	Kif18b	Cr
Cryab	Cd	Arsa	Cr	Klhl21	Cr
Ctgf	Cd	As3mt	Cr	Lin7c	Cr
Cyp3a9	Cd	Bcas3	Cr	Lrba	Cr
Dcbld2	Cd	Cacna1d	Cr	Lyar	Cr
Ddit3	Cd	Ccne2	Cr	Man1a1	Cr
Dnajb1	Cd	Cdh2	Cr	Mcm10	Cr
Fads3	Cd	Cdt1	Cr	Mcm3	Cr
Gadd45a	Cd	Chaf1b	Cr	Mcm5	Cr
Gadd45g	Cd	Cntf	Cr	Mcm6	Cr
Gbp2	Cd	Cohh1	Cr	Mcm7	Cr
Gng12	Cd	Cyp4f17	Cr	Mcm8	Cr
Gpr107	Cd	Ddx20	Cr	Mpnd	Cr
Grhl1	Cd	Dennd1a	Cr	Mybl2	Cr
Mdm2	Cd	Dock1	Cr	Mylk	Cr
Mllt11	Cd	Dst	Cr	Nat13	Cr
Mobkl1b	Cd	Elmo3	Cr	Ngef	Cr
Mx1	Cd	Ercc6l	Cr	Nqo1	Cr
Pmm1	Cd	Exo1	Cr	Nrbp2	Cr
Ppp1r15a	Cd	Exoc4	Cr	Nufip1	Cr

Table 4 (Continued): Candidate biomarker genes in the chemicals of interest.

Gene	Chemical	Gene	Chemical	Gene	Chemical
Nup85	Cr	Traip	Cr	Ero1l	Ni
Opn3	Cr	Uap1l1	Cr	Errfi1	Ni
Orc6l	Cr	Uchl5	Cr	Fasn	Ni
Osgin1	Cr	Uox	Cr	Fbxo30	Ni
Pcca	Cr	Usp1	Cr	Flot1	Ni
Pcna	Cr	Wee1	Cr	Gclc	Ni
Pftk1	Cr	Zfp367	Cr	Gjb1	Ni
Phf20l1	Cr	Cdr2	Cr, Cd	Grb14	Ni
Phlda1	Cr	Col18a1	Cr, Cd	Higd1a	Ni
Plcb1	Cr	Cps1	Cr, Cd	Hip1	Ni
Pold2	Cr	Lgals4	Cr, Cd	Ifitm3	Ni
Ptges2	Cr	Myo1g	Cr, Cd	Jmjd1a	Ni
Ptprd	Cr	Plg	Cr, Cd	Klf6	Ni
Ptprg	Cr	Ankrd37	Ni	Ldha	Ni
Qrich2	Cr	Apln	Ni	Map2k1	Ni
Rabgap1l	Cr	Arl6ip1	Ni	Mboat1	Ni
Rad51	Cr	Bcs1l	Ni	Nampt	Ni
Rad51ap1	Cr	BNip3	Ni	Nme3	Ni
RGD1303142	Cr	Btd	Ni	Nucb2	Ni
RGD1308772	Cr	C1s	Ni	P2ry2	Ni
RGD1559690	Cr	Cdh17	Ni	P4ha2	Ni
Rpa2	Cr	Chd6	Ni	Pbld	Ni
Rrm2	Cr	Chsy1	Ni	Pdk1	Ni
Senp7	Cr	Clcn4-2	Ni	Pgk1	Ni
Shank2	Cr	Cln3	Ni	Phyh	Ni
Skp2	Cr	Cpt1a	Ni	Pygl	Ni
Slc22a18	Cr	Creb3l1	Ni	Rfng	Ni
Slc25a21	Cr	Cxcl9	Ni	RGD1561455	Ni
Slc48a1	Cr	Dapl1	Ni	RGD1562059	Ni
Smoc1	Cr	Dcxr	Ni	Rnf217	Ni
Snd1	Cr	Ddit4	Ni	Rrbp1	Ni
Srebf1	Cr	DhCr24	Ni	Samd4a	Ni
Stard13	Cr	Egln1	Ni	Scly	Ni
Taf1d	Cr	Egln3	Ni	Stat1	Ni
Tle2	Cr	Elovl6	Ni	Stbd1	Ni

Table 4 (Continued): Candidate biomarker genes in the chemicals of interest.

Gene	Chemical
Sult1a1	Ni
Tes	Ni
Ttr	Ni
Txnrd1	Ni
Cbs	Ni
Ube2o	Ni
Ampd3	Ni, Cd
Anxa2	Ni, Cd
Cfi	Ni, Cd
Cxcl1	Ni, Cd
Dusp1	Ni, Cd
Emp1	Ni, Cd
Fetub	Ni, Cd
G6pc	Ni, Cd
Hspb8	Ni, Cd
Ifrd1	Ni, Cd
Jun	Ni, Cd
Obfc2a	Ni, Cd
Proc	Ni, Cd
RGD1566118	Ni, Cd
Rnd1	Ni, Cd
Slc30a1	Ni, Cd
Slc39a10	Ni, Cd
Sqstm1	Ni, Cd
Zyx	Ni, Cd
Akr1b8	Ni, Cr
C9	Ni, Cr
Calml4	Ni, Cr
Fam171a1	Ni, Cr
Fga	Ni, Cr
Hmgcs2	Ni, Cr
Map2k6	Ni, Cr
Pah	Ni, Cr
Rgn	Ni, Cr
Syne1	Ni, Cr
Wnk4	Ni, Cr

DISCUSSION

Nickel, chromium, and cadmium are heavy metals that have military, occupational, and environmental impacts. While the adverse effects of the metals have been well characterized, their exact mechanisms of toxicity have yet to be determined and few biomarkers exist for the early detection of an exposure. The metals are known to cause DNA damage, oxidative stress through the formation of reactive oxygen species, and/or interfere with normal cell biological and physiological processes. Gene expression studies were conducted, identifying 992 Affymetrix probe sets modulated as a result of exposure to nickel, chromium, or cadmium. The use of bioinformatic tools enabled the identification of pathways and functions with an over-representation of differentially expressed genes.

qPCR Validation

Validation of microarray data is a common practice since the quality of the data can vary with the platform and procedures used. Quantitative real-time PCR (qPCR) is a technique commonly used to validate microarray results. Correlations between the microarray and qPCR data were calculated using Pearson's correlation with results between 0.91 and 0.97. All genes used for validation that were changing by at least two fold due to a chemical exposure in the microarray results, were also changing by two fold in the same direction in the qPCR results. Since the fold changes were similar and the correlations were good, this will be considered a successful validation. The small discrepancies between the microarray and qPCR results may be due to the different efficiencies of the reverse transcription reactions, the differences in methods including

the hybridization step required only in microarray processing, or the different normalization techniques used by the different methods.

Candidate Biomarker Identification

Identifying and validating biomarkers for clinical use is a complex process. The first step, identifying differentially expressed genes for further investigation as candidate biomarkers, was undertaken as part of this project. Of the 992 probe sets differentially expressed in the H4IIE cell line as a result of exposure to at least one concentration of nickel, cadmium, and/or chromium, 246 were identified for further investigation for use as potential biomarkers. A biomarker does not need to be a single piece of data, but could be a panel that when taken as a whole provides useful information. A biomarker comprised of multiple pieces of information may more accurately examine biological processes on a system-wide scale (Aardema and MacGregor 2002). Therefore, these genes alone may not serve as a viable biomarker, but a group of them may serve as a fingerprint or signature of exposure. The differentially expressed genes were identified in one cell line and then validated in another to ensure the effects being seen were typical of the liver and likely to occur in whole animal systems as well. Further investigation and validation of the modulated probe sets is warranted as they were modulated in a rodent cell line and may not behave similarly *in vivo* in rodents or humans. To validate these gene transcripts for use as a biomarker of exposure or effect, the three metals would need to be tested in a rat whole animal system. The transcripts behaving similarly *in vivo* would also need to be tested in a human liver cell line to see if the genes are expressed as part of a highly conserved biological process before being validated in humans. Also, it

would need to be determined if the expression of the candidate biomarkers is detectable by minimally invasive procedures, such as through a blood sample, necessitating that the protein be expressed in a detectable manner, such as being secreted from the cell. No formal procedure for biomarker discovery exists, but these differentially expressed genes serve as a starting point and warrant further investigation and validation.

Chromium Toxicity Pathways

VxInsight, a data mining tool, was used to cluster probe sets with similar expression patterns among all the treatment groups. The white cluster was comprised of a total of 129 probe sets, 124 of which were differentially expressed due to chromium exposure and 8 were differentially expressed in nickel, 5 of which were unique only to nickel. Of the 5 probe sets not modulated in chromium, only 3 had annotation through Affymetrix (*Spc24, Tcf19, and Tk1*). Fifty-one of the 129 probes in the white cluster had no functional annotation. Therefore, it is possible to assign the effects observed in this cluster as a result of exposure to chromium, and allowing it to be used to investigate the mechanisms of toxicity of chromium.

The white cluster is dominated by genes involved in the DNA damage response suggesting a mechanism of toxicity for chromium (Figure 11). Of the 79 probe sets with functional annotation in the Affymetrix annotation file, 40 were placed in the DNA damage, replication, and repair bin base on GO terms. This is the most significantly enriched GO category of the entire data set. Chromium has been shown to cause DNA

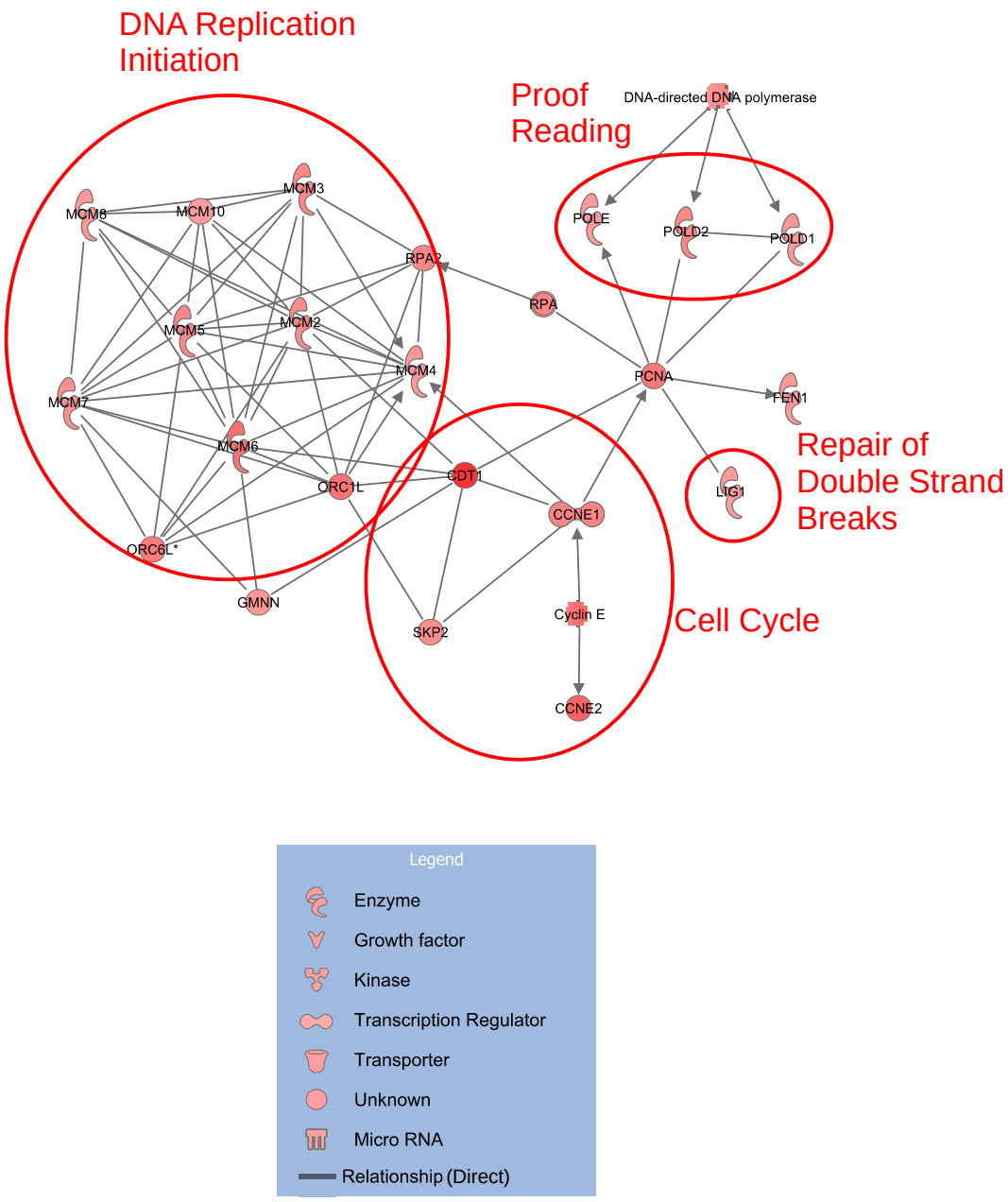

Figure 11: The presented image is a network of genes from the white cluster involved in the DNA damage response produced in IPA. The network displays the interaction between genes involved in DNA replication and repair among themselves and with genes involved in other biological functions such as cell cycle control. Genes with similar functions such as DNA replication initiation and double strand break repair are labeled as such. The intensity of the pink color represents the magnitude of the fold change, with a deeper the color representing a greater magnitude of change. Interactions are represented as lines with the direction of the arrow signifying the directionality of the interaction.

damage through the generation of ROS and by directly forming Cr-DNA adducts (Beyersmann and Hartwig 2008).

The up-regulation of genes involved in DNA replication and repair, such as DNA polymerases and those that make up the DNA synthesome, also suggest that chromium causes DNA damage (Bridgewater et al. 1998, Dai et al. 2009). The DNA synthesome is a multiprotein complex involved in DNA replication containing DNA polymerases α, δ (*Pold*), and ε (*Pole*), DNA primase, topoisomerases, proliferation cell nuclear antigen (*Pcna*), replication factor C (*Rfc*), replication protein A (*Rpa*), 3'>5' and 5'>3' DNA helicases, DNA methyltransferase, poly (ADP)-ribose polymerase and DNA ligase (Coll et al. 1996, Jiang et al. 2002). Many of the genes coding for the proteins in the DNA synthesome are differentially expressed in the white cluster including *Pcna*, *Rpa*, the minichromosome maintenance complex components which serve as helicases, *Pole*, and *Pold1*, providing a method through which the cells may be responding to the DNA damage caused by exposure to chromium.

The differentially expressed genes that make up part of the synthesome often play specific roles in DNA synthesis, suggesting more detailed mechanisms of toxicity. Since DNA polymerases δ and ε are associated with proof-reading and repair activity, their up-regulation may be in response to chromium specific DNA damage (Tran et al. 1999). DNA ligase is involved in repairing double strand breaks which are known to accumulate due to chromium toxicity. Some of the genes differentially expressed in the DNA synthesome, such as the minichromosome maintenance complex (MCM) and origin recognition complex (ORC), are involved specifically in the initiation of DNA synthesis

(Kawakami and Katayama 2010). It has been shown that Chromium-DNA adducts reduce the ability of synthesome to initiate replication (Dai et al. 2009); however these genes may be up-regulated as the cell attempts to repair damage caused by the chromium. Additionally, genes involved in excision repair to remove DNA adducts, such as *Rpa2*, *Pold*, and *Pcna*, were up-regulated in the white cluster suggesting that the direct interaction of Cr with DNA and the formation of adducts are involved in Cr toxicity.

The other biological process in the binning method that was significantly enriched in the white cluster was cell cycle. DNA replication and cell cycle control are thought to be closely associated (Sugimoto et al. 2004). In the G_1 phase, CDT1 is recruited to chromatin bound ORC functioning as a loader for the MCM complex, permitting the cell cycle to continue (Ishimi 1997, Sugimoto et al. 2004). Cyclin dependent kinases then repress the MCM's helicase activity in the S phase (Itzhaki et al. 1997). As these genes, including *Cdt1*, *Ccne1* which is a cyclin, and *Skp2*, a kinase, are up-regulated, the cells may have overcome cell cycle arrest as a survival technique for resistance to the toxic insult. Therefore, chromium toxicity may interfere with cell cycle regulation and induce the DNA replication machinery.

Nickel Toxicity Pathways

The blue cluster, as determined through VxInsight, contained 216 differentially expressed probe sets, 111 of which had no functional annotation provided by Affymetrix. Of the 216 differentially expressed probe sets only 4 were modulated only by Cr, 190 solely by Ni, 6 by both Ni and Cd, 14 by both Ni and Cr, and 2 by all three metals (Figure 12). In the binning methods, the oxidative stress, ion homeostasis, apoptosis, energy

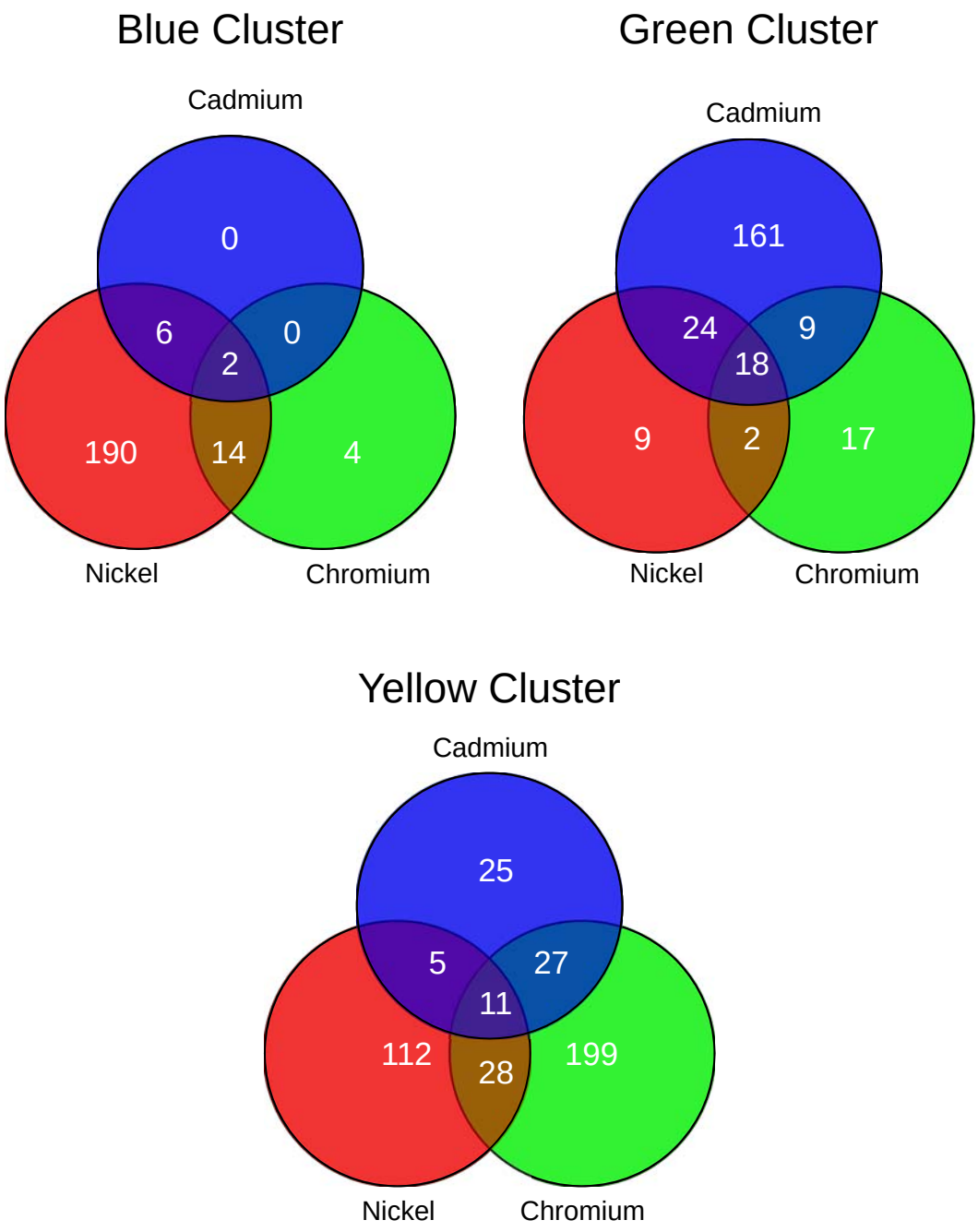

Figure 12: Venn diagram of differentially expressed probe sets in the blue cluster, green cluster, and yellow cluster as determined through cluster analysis using VxInsight. The blue cluster contains mostly probe sets modulated to exposure to nickel, the green cluster contains probe sets modulated in response to exposure to cadmium, and the yellow cluster is not specific to one chemical.

regulation, and hypoxic response categories were all enriched by the probe sets present in the blue cluster. Since all but four genes were differentially expressed in Ni, it is fair to consider effects observed in this cluster being a result of exposure to Ni and to use the blue cluster to investigate the mechanisms of toxicity of Ni.

Nickel is thought to cause toxicity by inducing the formation of reactive oxygen species (ROS) in a Fenton type reaction, catalyzing the generation of hydroxyl radicals from hydrogen peroxide causing damage to proteins and DNA (Beyersmann and Hartwig 2008). The ROS may also regulate transcription factors and signal transduction pathways involved in apoptosis and cell proliferation (Valko et al. 2005). Many genes involved in the oxidative stress response were up-regulated in the blue cluster, including, *Gpx1*, *Gclc*, *Ero1l*, *Aldh3a1*, *Loxl2*, and *Txnrd1*, suggesting that ROS play a role in nickel toxicity (Figure 13). Glutathione peroxidase 1 (*Gpx1)* is one of the most important antioxidant enzymes involved in the detoxification of hydrogen peroxide (Brigelius-Flohé 2006). Glutathione is an antioxidant known to prevent the nickel induced generation of ROS and the gene responsible for the first rate-limiting step in glutathione production, *Gclc*, was up-regulated in the blue bin (Das et al. 2008, Mascart and Gottignies 1979). *Ero1l* is involved in redox homeostasis and is induced in the course of the unfolded protein response (Pagani et al. 2000), and may therefore, be up-regulated in response to damaged proteins caused by oxidative stress. Aldehyde dehydrogenase 3A1 (*Aldh3a1*) plays multiple roles in protecting against oxidative stress such as scavenging ROS and perhaps reducing cell growth (Estey et al. 2007).

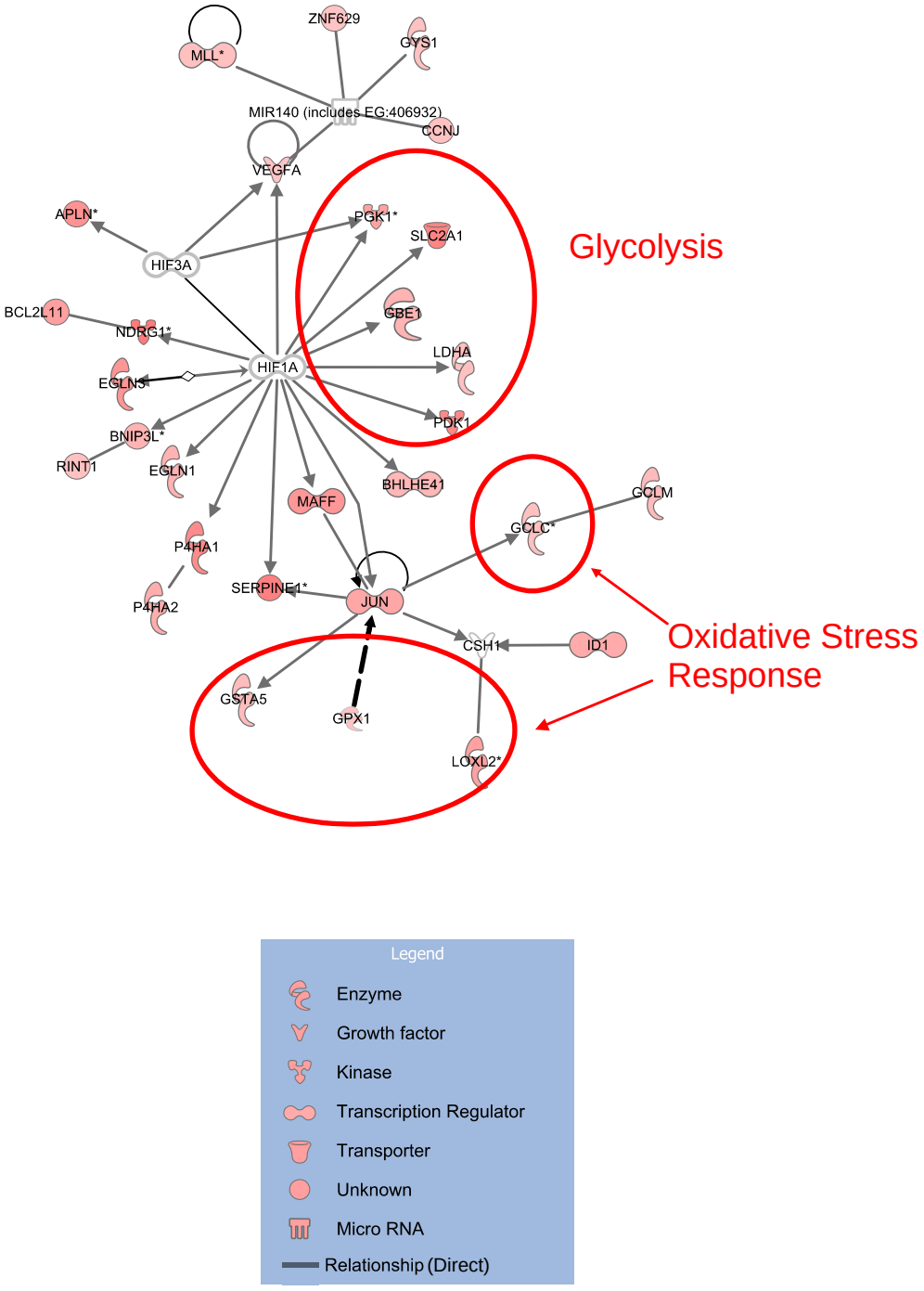

Figure 13: Network of genes from the blue cluster involved in the HIF-1α and oxidative stress response produced in IPA. Twenty-seven genes in this cluster are known to be regulated by HIF-1α. The intensity of the pink color represents the magnitude of the fold change, with a deeper the color representing a greater magnitude of the fold change. Interactions are represented as lines with the direction of the arrow signifying the directionality of the interaction.

Nickel has also been shown to activate the hypoxia-inducible factor-1α (HIF-1α) which induces the transcription of genes involved in glycolysis, glucose transport, apoptosis, and other cellular process (Beyersmann and Hartwig 2008). Nickel prevents the degradation of HIF-1α either by the depletion of ascorbate or by replacing iron in the hydroxylases responsible for HIF-1α degradation (Maxwell and Salnikow 2004, Salnikow et al. 2004). In the blue bin, 27 out of the 105 differentially expressed probe sets with annotation were HIF-1α regulated according to IPA, resulting in a significant enrichment of the HIF-1α canonical pathway in IPA, as well as the hypoxic response bin (Figure 13). Two functions regulated by HIF-1α, glycolysis and apoptosis, were also enriched by the differentially expressed probe sets in the blue cluster using the binning method. Genes involved in glycolysis are up-regulated as the cell begins to use glucose as the main energy source in the absence of oxygen or HIF-1α activation (Marín-Hernández et al. 2009, Semenza 2007).

As a result of mimicking hypoxia and the activation of HIF-1α, many of the genes involved in aerobic energy production would be expected to be down-regulated while increasing glycolysis. The biological functions lipid and carbohydrate metabolism were down regulated overall in the yellow cluster, a trend continued when only the nickel modulated genes were observed. For example, genes involved in lipid metabolism such as *Mgll* and *Cpt1a* are down regulated in the yellow cluster by nickel only.

The biological processes modulated by the genes in the blue cluster suggest two main methods through which nickel may exert its toxicity. Genes involved in apoptosis and glycolysis, processes regulated by both ROS and HIF-1α, are differentially expressed

in this cluster. Both these pathways may contribute to nickel toxicity, but further investigation is warranted to determine the involvement of each.

Cadmium Toxicity Pathways

The green cluster, as determined through VxInsight, contained a total of 240 probe sets, only 154 of which had functional annotation provided by Affymetrix. Of the 240 probe sets modulated in this cluster, 18 of the probe sets were differentially expressed by all three chemicals, 161 by Cd only, 9 by Cd and Cr, 24 by Ni and Cd, 17 by Cr only, 2 by Ni and Cr, and 9 by only Ni (Figure 12). Therefore, taking into account that only a few of these probe set are not differentially expressed as a result of exposure to Cd, the green cluster could be seen as probe sets that respond to Cd and be used to investigation the mechanisms of toxicity of Cd.

Many of the genes in the green cluster and differentially expressed due to exposure to Cd may have been up-regulated through p53 activation (Figure 14). Cadmium has been shown to induce apoptosis through the activation of p53-mediated signaling (Son et al. 2010). Many genes regulated by p53 and involved in apoptosis, such as Casp4, Abcb1, and Mdm2, are up-regulated in the green cluster and due to cadmium intoxication. Additionally, biological processes such as cell cycle, cell death, and p53 signaling were enriched by probe sets in the green cluster as observed in IPA analysis and the binning method.

Other genes in the green cluster and modulated by Cd, such as heat shock proteins (HSP) may be involved in general stress. Heat shock proteins are cellular chaperone

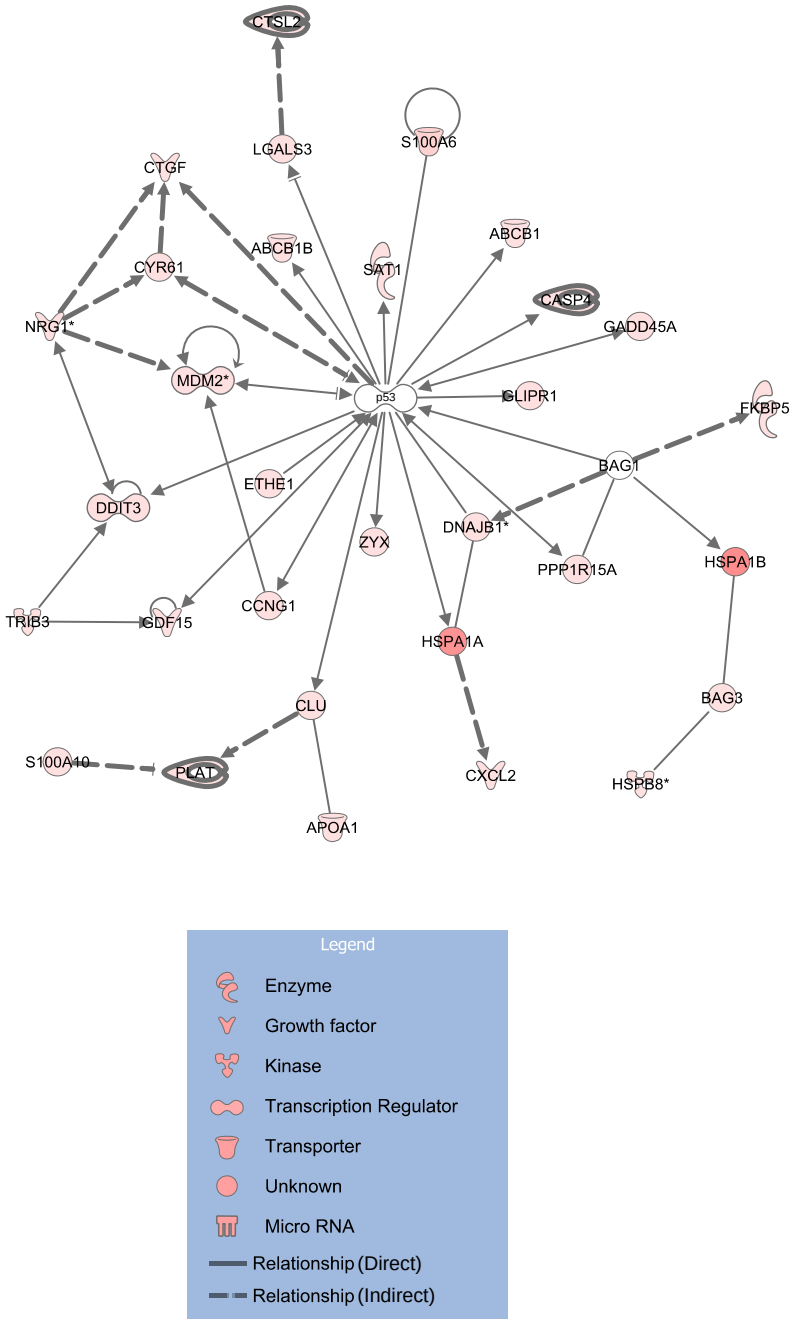

Figure 14: Network of genes, produced with IPA, differentially expressed in the green cluster and as a result of exposure to cadmium. Most of these genes are involved in apoptosis and are regulated by p53, suggesting that Cd induces p53-mediated apoptosis. The intensity of the pink color represents the magnitude of the fold change, with a deeper the color representing a greater magnitude of the change. Interactions are represented as lines with the direction of the arrow signifying the directionality of the interaction.

proteins involved in the folding and degradation of proteins as well as apoptosis (Bertin and Averbeck 2006). Cadmium has been shown to up-regulate HSP (Escobar et al. 2009) which may be responding to the protein damage caused by oxidative stress. In the green cluster, heat shock proteins such as *Hspa1a*, *Hspa1b*, and *Hspb8* were differentially expressed, suggesting that Cd induced oxidative stress may cause protein degradation

Effects Common to Nickel, Chromium, and Cadmium

Eighteen of the probe sets in the green cluster are differentially expressed in all three chemical exposures. The genes in this group are comprised mostly of those involved in general and oxidative stress or metal response such as heme oxygenase 1 (*Hmox1*), metallothionein 1a and 2a (*Mt1a* and *Mt2a*), and activating transcription factor 3 (*Atf3*). *Hmox1* is a ubiquitous stress response protein involved in reducing the effects of oxidative stress and apoptosis (Ryter and Choi 2009). Metallothioneins are involved in the transport and detoxification of heavy metals and protection against oxidative stress (Krizkova et al. 2009). *Atf3* is a transcription factor whose expression has been shown to increase in response to stress (Hai et al. 1999).

Additionally, the yellow cluster contains 11 probe sets differentially expressed due to exposure to all three of the chemicals tested. Four hundred-seven probe sets were down regulated throughout all three metals; 156 in nickel, 265 in chromium, and 68 in cadmium, with some overlap between the chemicals (Figure 12). Many of the genes in this cluster may be down regulated in response to oxidative stress, as that bin was significantly enriched. For example, Glutaredoxin-1 (GLRX), a protein whose activity has been shown to be decreased by both hydrogen peroxide and cadmium, is involved in

apoptosis and the oxidative stress response. Also, many of the genes in the yellow cluster, such as *Ctnnb1*, *Itgb1*, cadherins *Cdh2* and *Cdh17*, are involved in cell adhesion (Prozialeck et al. 2002). These genes may be down regulated as a result of the cells detaching from the surface and each other as a result of apoptosis and interruption of the cell cycle.

Interestingly, using the binning method for the yellow cluster resulted in two bins being significant as a result of containing fewer genes than expected than by chance alone. This may be less of a result of biological function and more of a result of the method used. The two bins that contained significantly fewer genes than expected were the DNA damage, replication, and repair and the cell cycle bin. It is possible that since these two bins, especially DNA damage, replication and repair, were so strongly enriched in other clusters that not as many probe sets would have been available to enrich those bins in the yellow cluster.

Future Directions

While microarray analysis suggests toxicity pathways involved in nickel, chromium, and cadmium intoxication, hard conclusions about the exact mechanisms cannot be made without further investigation. This project has suggested that the DNA repair and replication process has been affected by chromium, perhaps through disruption of the DNA synthesome or directly damaging the DNA. Since Cr produces ROS and forms Cr-DNA adducts, microarray analysis alone cannot determine the extent to which each plays a role in Cr toxicity and DNA damage. Studies using a ROS scavenger to remove oxidative stress may be useful in determining the role the two mechanisms play

in chromium toxicity. Similarly, many of the differentially expressed genes as a result of exposure to nickel may be controlled by the transcription factor HIF-1α. However, microarray technology cannot detect HIF-1α activation since HIF-1α is regulated at the protein level, and nickel blocks its degradation. A western blot could be used to measure the amount of the HIF-1α in cells exposed to nickel to see if the protein is stabilized.

The extensive data gathered not only provides many avenues of exploration, but also complicates the analysis itself. Hundreds of bioinformatic tools are available to decipher the biological meaning of microarray experiments, however none are perfect. In this project IPA, GOTM, VxInsight, and others initially used for initial data exploration were used for analysis. These packages cover free, web-based applications to commercial, manually curated software packages. While these tools do aid in annotation and exploration, especially when applying statistical significance, nothing replaces intensive manual annotation and investigation.

Additionally, 992 probe sets were identified as differentially expressed; however, only roughly a third of them had any functionally annotation through current bioinformatic methods. The genes without annotation provide another opportunity for further investigation as they may play significant, and currently unknown, roles in the cell's response to Ni, Cr, and Cd. Since many of these unknown gene transcripts clustered with genes of known function, they may have similar roles or be regulated by the same mechanisms. Basic Local Alignment Search Tool (BLAST) could be used to determine if the sequences of these probe sets are homologous to any known genes or if

their promoter sequences contain binding sites for the same transcription factors, suggesting similar control mechanisms (Altschul et al. 1990).

Conclusion

Nickel, chromium, and cadmium are heavy metals found in the military, industry, and the environment that have adverse health effects on individuals exposed to them. While the mechanisms of toxicity of the metals are not completely understood, it is thought that they have similar effects, but with different pathways. In order to investigate the effects of these metals and to investigate possible biomarkers, cells were treated with nickel, chromium, or cadmium and the gene expression patterns were measured using microarray technology. A total of 992 unique probe sets were differentially expressed as a result of treatment to nickel, chromium, or cadmium, suggesting unique molecular mechanisms of action for each metal.

Genes whose transcripts were differentially expressed in both the H4IIE and MH1C1 cell line were identified as genes of interest for further investigation as biomarkers. A total of 246 genes with known functions were modulated similarly in both cell lines. Identifying the genes of interest in one rat liver-derived cell line, and validating the changes in another rat liver-derived cell line ensured that the results were reflective of hepatocyte-like function.

Bioinformatic tools were used to determine biological functions affected by exposure to nickel, chromium, and/or cadmium. The 992 differentially expressed probe sets were shown to be involved in such biological processes as oxidative stress response,

interference with the cell cycle, and apoptosis. All three metals increased the expression of genes in response to general and metal stress, such as *Atf1* and metallothioneins, and oxidative stress, such as *Hmox*. Chromium is the only metal of the three to directly interact and cause damage to DNA, as observed with the heavily enriched DNA damage, replication, and repair bin of the white cluster. Nickel was shown to induce oxidative stress, and interfere with energy production and induce apoptosis perhaps through HIF-1α signaling. Cadmium increased expression of genes as a result of oxidative stress such as the HSPs and caused activation of the p53 pathway inducing cell cycle arrest and apoptosis.

In conclusion, the gene expression of two rat liver hepatoma cell lines were investigated to discover candidate biomarkers of exposure and effect and identify possible mechanism of toxicity of nickel, chromium, and cadmium. A total of 992 unique differentially expressed probe sets were identified, 246 of which are reproducible and may be further investigated as possible biomarkers of effect for the chemicals. Potential mechanisms of toxicity with unique molecular modes of action were identified for the metals including oxidative stress, DNA damage, and/or hypoxia, providing avenues for further investigation.

REFERENCES

Aardema MJ, MacGregor JT. 2002. Toxicology and genetic toxicology in the new era of "toxicogenomics": impact of "-omics" technologies. *Mutation Research*. 499(1): 13-25.

Agency for Toxic Substances and Disease Registry (ATSDR). 2005a. Toxicological profile for nickel. Atlanta, GA: U.S. Department of Health and Human Services, Public Health Service.

Agency for Toxic Substances and Disease Registry (ATSDR). 2005b. Hazardous Substances Emergency Events Surveillance System. Atlanta, GA: U.S. Department of Health and Human Services, Public Health Service.

Altschul SF, Gish W, Miller W, Myers EW, Lipman DJ. 1990. Basic local alignment search tool. *Journal of Molecular Biology*. 215(3):403–410.

Archer KJ, Reese SE. 2010. Detection call algorithms for high-throughput gene expression microarray data. *Briefings in Bioinformatics*. 11(2): 244-252.

Arikawa E, Sun Y, Wang J, Zhou Q, Ning B, Dial SL, Guo L, Yang J. 2008. Cross-platform comparison of SYBR Green real-time PCR with TaqMan PCR, microarrays and other gene expression measurement technologies evaluated in the MicroArray Quality Control (MAQC) study. *BMC Genomics* 9: 328.

Barceloux D G. 1999. Chromium. *Journal of Toxicology. Clinical Toxicology* 37(2): 173-194.

Benjamini Y, Hochberg Y. 1995. Controlling the False Discovery Rate: A Practical and Powerful Approach to Multiple Testing. *Journal of the Royal Statistical Society. Series B (Methodological)* 57(1): 300, 289.

Bertin G, Averbeck D. 2006. Cadmium: cellular effects, modifications of biomolecules, modulation of DNA repair and genotoxic consequences (a review). *Biochimie* 88(11): 1549-1559.

Beyersmann D, Hartwig A. 2008. Carcinogenic metal compounds: recent insight into molecular and cellular mechanisms. *Archives of Toxicology* 82(8): 493-512.

Boyack KW, Wylie BN, Davidson GS. 2002. Domain Visualization using VxInsight for science and technology management. *Journal of the American Society for Information Science and Technology* 53(9): 764-774.

Bridgewater LC, Manning FC, Patierno SR. 1998. Arrest of replication by mammalian DNA polymerases alpha and beta caused by chromium-DNA lesions. *Molecular Carcinogenesis* 23(4): 201-206.

Brigelius-Flohé R. 2006. Glutathione peroxidases and redox-regulated transcription factors. *Biological Chemistry* 387(10-11): 1329-1335.

Canales RD, Luo Y, Willey JC, Austermiller B, Barbacioru CC, Boysen C, Hunkapiller K, Jensen RV, Knight CR, Lee KY, Ma Y, Maqsodi B, Papallo A, Peters EH, Poulter K, Ruppel PL, Samaha RR, Shi L, Yang W, Zhang L, Goodsaid FM. 2006. Evaluation of DNA microarray results with quantitative gene expression platforms. *Nature Biotechnology* 24(9): 1115-1122.

Coll JM, Sekowski JW, Hickey RJ, Schnaper L, Yue W, Brodie AM, Uitto L, Syvaoja JE, Malkas LH. 1996. The human breast cell DNA synthesome: its purification from tumor tissue and cell culture. *Oncology Research* 8(10-11): 435-447.

Dai H, Liu J, Malkas LH, Catalano J, Alagharu S, Hickey RJ. 2009. Chromium reduces the in vitro activity and fidelity of DNA replication mediated by the human cell DNA synthesome. *Toxicology and Applied Pharmacology* 236(2): 154-165.

Dalmasso E. 2008. Planning for Success in Biomarker Disocery. *Genetic Engineering & Biotechnology News* 28(12).

Das KK, Das SN, and Dhundasi SA. 2008. Nickel, its adverse health effects & oxidative stress. *The Indian Journal of Medical Research* 128(4): 412-425.

Dounce AL, Lan TH. 1943. ISOLATION AND PROPERTIES OF CHICKEN ERYTHROCYTE NUCLEI. *Science (New York, N.Y.)* 97(2530): 584-585.

Escobar Mdel C, Souza V, Bucio L, Hernández E, Gómez-Quiroz LE, Gutiérrez Ruiz MC. 2009. MAPK activation is involved in cadmium-induced Hsp70 expression in HepG2 cells. *Toxicology Mechanisms and Methods* 19(8): 503-509.

Estey T, Piatigorsky J, Lassen N, Vasiliou V. 2007. ALDH3A1: a corneal crystallin with diverse functions. *Experimental Eye Research* 84(1): 3-12.

Hai T, Wolfgang CD, Marsee DK, Allen AE, Sivaprasad U. 1999. ATF3 and stress responses. *Gene Expression* 7(4-6): 321-335.

Irizarry RA, Hobbs B, Collin F, Beazer-Barclay YD, Antonellis KJ, Scherf U, Speed TP. 2003. Exploration, normalization, and summaries of high density oligonucleotide array probe level data. *Biostatistics (Oxford, England)* 4(2): 249-264.

Ishimi, Y. 1997. A DNA helicase activity is associated with an MCM4, -6, and -7 protein complex. *The Journal of Biological Chemistry* 272(39): 24508-24513.

Itzhaki JE, Gilbert CS, Porter AC. 1997. Construction by gene targeting in human cells of a conditional' CDC2 mutant that rereplicates its DNA. *Nature Genetics* 15(3): 258-265.

Jiang HY, Hickey RJ, Abdel-Aziz W, Tom TD, Wills PW, Liu J, Malkas LH. 2002. Human cell DNA replication is mediated by a discrete multiprotein complex. *Journal of Cellular Biochemistry* 85(4): 762-774.

Kalinich JF, Emond CA, Dalton TK, Mog SR, Coleman GD, Kordell JE, Miller AC, McClain DE. 2005. Embedded weapons-grade tungsten alloy shrapnel rapidly induces metastatic high-grade rhabdomyosarcomas in F344 rats. *Environmental Health Perspectives* 113(6): 729-734.

Kawakami H, Katayama T. 2010. DnaA, ORC, and Cdc6: similarity beyond the domains of life and diversity. *Biochemistry and Cell Biology = Biochimie Et Biologie Cellulaire* 88(1): 49-62.

Kim SK, Lund J, Kiraly M, Duke K, Jiang M, Stuart JM, Eizinger A, Wylie BN, Davidson GS. 2001. A gene expression map for Caenorhabditis elegans. *Science* 293(5537): 2087-2092.

Krizkova S, Fabrik I, Adam V, Hrabeta J, Eckschlager T, Kizek R. 2009. Metallothionein--a promising tool for cancer diagnostics. *Bratislavské Lekárske Listy* 110(2): 93-97.

Livak KJ, Schmittgen TD. 2001. Analysis of relative gene expression data using real-time quantitative PCR and the 2(-Delta Delta C(T)) Method. *Methods (San Diego, Calif.)* 25(4): 402-408.

Marín-Hernández A, Gallardo-Pérez JC, Ralph SJ, Rodríguez-Enríquez S, Moreno-Sánchez R. 2009. HIF-1alpha modulates energy metabolism in cancer cells by inducing over-expression of specific glycolytic isoforms. *Mini Reviews in Medicinal Chemistry* 9(9): 1084-1101.

Mascart G, Gottignies P. 1979. Enteritis and septicaemia due to Campylobacter jejuni. *Acta Clinica Belgica* 34(6): 365-369.

Maxwell P, Salnikow K. 2004. HIF-1: an oxygen and metal responsive transcription factor. *Cancer Biology & Therapy* 3(1): 29-35.

McKone TE, Huey BM, Downing E, Duffy LM. 2000. Chemical Warfare Agents. In: Strategies to Protect the Health of Deployed U.S. Forces. Washington, D.C.: National Academy Press. p. 53-56.

Meo SA, Al-Khlaiwi T. 2003. Health hazards of welding fumes. *Saudi Medical Journal* 24(11): 1176-1182.

Michels G, Wätjen W, Weber N, Niering P, Chovolou Y, Kampkötter A, Proksch P, Kahl R. 2006. Resveratrol induces apoptotic cell death in rat H4IIE hepatoma cells but necrosis in C6 glioma cells. *Toxicology* 225(2-3): 173-182.

Morey JS, Ryan JC, Van Dolah FM. 2006. Microarray validation: factors influencing correlation between oligonucleotide microarrays and real-time PCR. *Biological Procedures Online* 8: 175-193.

Odashima S, Nakayabu Y, Honjo N, Abe H, Arichi S. 1979. Induction of phenotypic reverse transformation by ginsenosides in cultured Morris hepatoma cells. *European Journal of Cancer* 15(6): 885-892.

Pagani M, Fabbri M, Benedetti C, Fassio A, Pilati S, Bulleid NJ, Cabibbo A, Sitia R. 2000. Endoplasmic reticulum oxidoreductin 1-lbeta (ERO1-Lbeta), a human gene induced in the course of the unfolded protein response. *The Journal of Biological Chemistry* 275(31): 23685-23692.

Prozialeck WC, Grunwald GB, Dey PM, Reuhl KR, Parrish AR. 2002. Cadherins and NCAM as potential targets in metal toxicity. *Toxicology and Applied Pharmacology* 182(3): 255-265.

Pruitt KD, Tatusova, T, Maglott DR. 2007. NCBI Reference Sequence (RefSeq): a curated non-redundant sequence database of genomes, transcripts, and proteins. *Nucleic Acid Research*. 35: D61-65.

Ryter SW, Choi AMK. 2009. Heme oxygenase-1/carbon monoxide: from metabolism to molecular therapy. *American Journal of Respiratory Cell and Molecular Biology* 41(3): 251-260.

Salnikow K, Donald SP, Bruick RK, Zhitkovich A, Phang JM, Kasprzak KS. 2004. Depletion of intracellular ascorbate by the carcinogenic metals nickel and cobalt results in the induction of hypoxic stress. *The Journal of Biological Chemistry* 279(39): 40337-40344.

Semenza GL. 2007. Oxygen-dependent regulation of mitochondrial respiration by hypoxia-inducible factor 1. *The Biochemical Journal* 405(1): 1-9.

Son YO, Lee JC, Hitron JA, Pan J, Zhang Z, Shi X. 2010. Cadmium induces intracellular Ca2+- and H2O2-dependent apoptosis through JNK- and p53-mediated pathways in skin epidermal cell line. *Toxicological Sciences: An Official Journal of the Society of Toxicology* 113(1): 127-137.

Stohs SJ, Bagchi D, Hassoun E, Bagchi M. 2001. Oxidative mechanisms in the toxicity of chromium and cadmium ions. *Journal of Environmental Pathology, Toxicology and Oncology: Official Organ of the International Society for Environmental Toxicology and Cancer* 20(2): 77-88.

Sugimoto N, Tatsumi Y, Tsurumi T, Matsukage A, Kiyono T, Nishitani H, Fujita M. 2004. Cdt1 phosphorylation by cyclin A-dependent kinases negatively regulates its function without affecting geminin binding. *The Journal of Biological Chemistry* 279(19): 19691-19697.

The Associated Press. 2009. Oregon: Possible Chemical Exposure. *The New York Times*. Available at: http://www.nytimes.com/2009/02/12/us/12brfs-POSSIBLECHEM_BRF.html [Accessed February 4, 2010].

Tran HT, Gordenin DA, Resnick MA. 1999. The 3'-->5' exonucleases of DNA polymerases delta and epsilon and the 5'-->3' exonuclease Exo1 have major roles in postreplication mutation avoidance in Saccharomyces cerevisiae. *Molecular and Cellular Biology* 19(3): 2000-2007.

U.S.Army Center for Health Promotion and Preventive Medicine. 2008. Just the Facts...Toxic Industrial Chemicals - Medical.

U.S.Department of Health and Human Services, Food and Drug Administration, Center for Drug Evalutaion and Research, & Center for Biologics Evaluation and Research (2008). E15 Definitions for Genomic Biomarkers, Pharmacogenomics, Pharmacogenetics,Genomic Data and Sample Coding Categories. Rockville, MD.

Valko M, Morris H, Cronin MTD. 2005. Metals, toxicity and oxidative stress. *Current Medicinal Chemistry* 12(10): 1161-1208.

Zhang B, Schmoyer D, Kirov S, Snoddy J. 2004. GOTree Machine (GOTM): a web-based platform for interpreting sets of interesting genes using Gene Ontology hierarchies. *BMC Bioinformatics* 5: 16.

APPENDIX 1: GO TERMS FOR BIN CATEGORIES

DNA Damage, Replication, and Repair
base-excision repair, DNA ligation
cellular response to DNA damage stimulus
DNA catabolic process
DNA catabolic process, exonucleolytic
DNA damage checkpoint
DNA damage response, detection of DNA damage
DNA damage response, signal transduction
DNA damage response, signal transduction by p53 class mediator
DNA damage response, signal transduction by p53 class mediator resulting in cell cycle arrest
DNA damage response, signal transduction by p53 class mediator resulting in induction of apoptosis
DNA damage response, signal transduction by p53 class mediator resulting in transcription of p21 class mediator
DNA damage response, signal transduction resulting in induction of apoptosis
DNA dealkylation
DNA double-strand break processing
DNA duplex unwinding
DNA integration
DNA ligation
DNA metabolic process
DNA methylation
DNA methylation on cytosine within a CG sequence
DNA recombination
DNA repair
DNA replication
DNA replication checkpoint
DNA replication initiation
DNA replication proofreading
DNA replication, synthesis of RNA primer
DNA synthesis during DNA repair
DNA topological change
DNA unwinding during replication
DNA-dependent DNA replication
error-prone postreplication DNA repair
intra-S DNA damage checkpoint
maintenance of DNA methylation
maintenance of DNA repeat elements
mitochondrial DNA replication
negative regulation of DNA binding
negative regulation of DNA recombination
negative regulation of DNA repair

APPENDIX 1 (CONTINUED)

DNA Damage, Replication, and Repair (Continued)

negative regulation of DNA replication
negative regulation of transcription from RNA polymerase II promoter in response to UV-induced DNA damage
nucleotide-excision repair, DNA damage removal
nucleotide-excision repair, DNA duplex unwinding
nucleotide-excision repair, DNA gap filling
nucleotide-excision repair, DNA incision, 3'-to lesion
nucleotide-excision repair, DNA incision, 5'-to lesion
positive regulation of DNA binding
positive regulation of DNA damage response, signal transduction by p53 class mediator
positive regulation of DNA ligation
positive regulation of DNA repair
positive regulation of DNA replication
regulation of DNA binding
regulation of DNA recombination
regulation of DNA replication
regulation of DNA replication initiation
response to DNA damage stimulus
M transition DNA damage checkpoint
M transition DNA damage checkpoint
centromeric heterochromatin formation
ATP-dependent chromatin remodeling
chromatin assembly or disassembly
chromatin modification
chromatin remodeling
chromatin silencing
chromatin silencing at telomere
chromosome condensation
chromosome organization
chromosome segregation
establishment or maintenance of chromatin architecture
methylation-dependent chromatin silencing
regulation of chromatin assembly or disassembly
ATP-dependent chromatin remodeling
nucleobase, nucleoside, nucleotide and nucleic acid metabolic process
cyclic nucleotide biosynthetic process
deoxyribonucleotide biosynthetic process
deoxyribonucleotide catabolic process
deoxyribonucleotide metabolic process
cyclic nucleotide catabolic process
negative regulation of nucleotide metabolic process
nucleotide phosphorylation

APPENDIX 1 (CONTINUED)

DNA Damage, Replication, and Repair (Continued)
nucleotide-excision repair
nucleotide-excision repair, DNA damage removal
nucleotide-excision repair, DNA duplex unwinding
nucleotide-excision repair, DNA gap filling
nucleotide-excision repair, DNA incision, 3'-to lesion
nucleotide-excision repair, DNA incision, 5'-to lesion
purine nucleotide biosynthetic process
purine nucleotide metabolic process
purine ribonucleotide biosynthetic process
purine ribonucleotide transport
pyridine nucleotide biosynthetic process
transcription-coupled nucleotide-excision repair

Cell Cycle
DNA damage response, signal transduction by p53 class mediator resulting in cell cycle arrest
G1 phase of mitotic cell cycle
G2 phase of mitotic cell cycle
M phase of mitotic cell cycle
meiotic cell cycle
mitotic cell cycle
mitotic cell cycle checkpoint
mitotic cell cycle G2
mitotic cell cycle spindle assembly checkpoint
negative regulation of cell cycle
negative regulation of mitotic cell cycle
negative regulation of S phase of mitotic cell cycle
positive regulation of cell cycle
re-entry into mitotic cell cycle
regulation of cell cycle
regulation of mitotic cell cycle
regulation of S phase of mitotic cell cycle
S phase of mitotic cell cycle
traversing start control point of mitotic cell cycle
M transition of mitotic cell cycle
S transition of mitotic cell cycle
cell cycle
cell cycle arrest
cell cycle checkpoint
cell cycle process
cell proliferation
negative regulation of cell proliferation

APPENDIX 1 (CONTINUED)

Cell Cycle (Continued)
positive regulation of cell proliferation
regulation of cell proliferation
general transcription from RNA polymerase II promoter
negative regulation of gene-specific transcription
negative regulation of transcription
negative regulation of transcription from RNA polymerase II promoter
negative regulation of transcription from RNA polymerase III promoter
negative regulation of transcription, DNA-dependent
positive regulation of gene-specific transcription
positive regulation of specific transcription from RNA polymerase II promoter
positive regulation of specific transcription from RNA polymerase II promoter
positive regulation of transcription from RNA polymerase I promoter
positive regulation of transcription from RNA polymerase II promoter
positive regulation of transcription from RNA polymerase II promoter, global
positive regulation of transcription, DNA-dependent
regulation of transcription
regulation of transcription from RNA polymerase I promoter
regulation of transcription from RNA polymerase II promoter
regulation of transcription, DNA-dependent
regulation of transcriptional preinitiation complex assembly
regulation of transcriptional preinitiation complex assembly
transcription
transcription from RNA polymerase I promoter
transcription from RNA polymerase II promoter
transcription from RNA polymerase III promoter
transcription initiation
transcription initiation from RNA polymerase I promoter
transcription initiation from RNA polymerase II promoter
transcription of nuclear rRNA large RNA polymerase I transcript
transcription termination
transcription, DNA-dependent
transcriptional preinitiation complex assembly

Oxidative Stress
heme oxidation
induction of apoptosis by oxidative stress
NADH oxidation
negative regulation of plasma lipoprotein oxidation
oxidation reduction
oxidative phosphorylation
regulation of transcription from RNA polymerase II promoter in response to oxidative stress

APPENDIX 1 (CONTINUED)

Oxidative Stress (Continued)
response to oxidative stress
cell redox homeostasis
redox signal response
hydrogen peroxide catabolic process
removal of superoxide radicals
response to hydrogen peroxide
response to superoxide
removal of superoxide radicals
response to oxygen radical
glutathione biosynthetic process
glutathione metabolic process
transmembrane glutathione transport

Ion Homeostasis
response to zinc ion
sodium ion transport
transition metal ion transport
zinc ion transport
calcium ion homeostasis
calcium ion transport
cellular calcium ion homeostasis
cellular chloride ion homeostasis
cellular iron ion homeostasis
cellular metal ion homeostasis
cellular potassium ion homeostasis
cellular response to iron ion starvation
cellular response to potassium ion starvation
cellular sodium ion homeostasis
cellular zinc ion homeostasis
cobalt ion transport
cytosolic calcium ion homeostasis
detection of calcium ion
elevation of cytosolic calcium ion concentration
endoplasmic reticulum calcium ion homeostasis
ion transport
iron ion homeostasis
iron ion transport
magnesium ion transport
manganese ion transport
metal ion transport
mitochondrial calcium ion transport
mitochondrial iron ion transport

APPENDIX 1 (CONTINUED)

Ion Homeostasis (Continued)
negative regulation of sodium ion transport
nickel ion transport
positive regulation of calcium ion transport
positive regulation of calcium ion transport into cytosol
positive regulation of calcium ion transport via store-operated calcium channel activity
positive regulation of potassium ion transport
positive regulation of sodium ion transport
potassium ion import
potassium ion transport
reduction of cytosolic calcium ion concentration
regulation of sodium ion transport

Apoptosis
anti-apoptosis
apoptosis
apoptosis in response to endoplasmic reticulum stress
DNA damage response, signal transduction by p53 class mediator resulting in induction of apoptosis
DNA damage response, signal transduction resulting in induction of apoptosis
DNA fragmentation involved in apoptosis
induction of apoptosis
induction of apoptosis by extracellular signals
induction of apoptosis by intracellular signals
induction of apoptosis by oxidative stress
induction of apoptosis via death domain receptors
negative regulation of anti-apoptosis
negative regulation of apoptosis
positive regulation of anti-apoptosis
positive regulation of apoptosis
protein insertion into mitochondrial membrane during induction of apoptosis
regulation of anti-apoptosis
regulation of apoptosis
transformed cell apoptosis
activation of pro-apoptotic gene products
cell death
death
positive regulation of programmed cell death
programmed cell death

Energy regulation
cellular glucose homeostasis
glucose 1-phosphate metabolic process

APPENDIX 1 (CONTINUED)

Energy Regulation (Continued)
glucose 6-phosphate metabolic process
glucose catabolic process
glucose homeostasis
glucose metabolic process
glucose transport
glucose-6-phosphate transport
negative regulation of glucose import
positive regulation of glucose import
glycolysis
regulation of glycolysis

Hypoxic response
response to hypoxia

APPENDIX 2: PROBE SETS DIFFERENTIALLY EXPRESSED BY NICKEL

Affymetrix ID	Gene Symbol	Gene Title	Cluster
1367576_at	Gpx1	glutathione peroxidase 1	Blue
1367586_at	Ldha	lactate dehydrogenase A	Blue
1367603_at	Tpi1	triosephosphate isomerase 1	Blue
1367705_at	Glrx1	glutaredoxin 1 (thioltransferase)	Yellow
1367707_at	Fasn	fatty acid synthase	Yellow
1367708_a_at	Fasn	fatty acid synthase	Yellow
1367722_at	Dpp7	dipeptidylpeptidase 7	Yellow
1367754_s_at	Asl	argininosuccinate lyase	Yellow
1367758_at	Afp	alpha-fetoprotein	Yellow
1367760_at	Map2k1	mitogen activated protein kinase kinase 1	Blue
1367775_at	Amacr	alpha-methylacyl-CoA racemase	Yellow
1367786_at	Psmb8	proteasome (prosome, macropain) subunit, beta type 8	Yellow
1367866_at	Fbln5	fibulin 5	Yellow
1367898_at	Bnip3l	BCL2/adenovirus E1B interacting protein 3-like	Blue
1367901_at	Gusb	glucuronidase, beta	Yellow
1368000_at	C3	complement component 3	Blue
1368025_at	Ddit4	DNA-damage-inducible transcript 4	Blue
1368079_at	Pdk1	pyruvate dehydrogenase kinase, isozyme 1	Blue
1368082_at	Slc4a2	solute carrier family 4 (anion exchanger), member 2	Yellow
1368130_at	Aldh3a1	aldehyde dehydrogenase 3 family, member A1	Blue
1368174_at	Egln3	EGL nine homolog 3 (C. elegans)	Blue
1368241_a_at	Flot1	flotillin 1	Yellow
1368258_at	Apln	apelin	Blue
1368280_at	Ctsc	cathepsin C	Yellow
1368308_at	Myc	myelocytomatosis oncogene	Blue
1368428_at	Xpnpep2	X-prolyl aminopeptidase (aminopeptidase P) 2, membrane-bound	Yellow
1368488_at	Nfil3	nuclear factor, interleukin 3 regulated	Blue
1368511_at	Bhlhe41	basic helix-loop-helix family, member e41	Blue
1368519_at	Serpine1	serine (or cysteine) peptidase inhibitor, clade E, member 1	Blue
1368618_at	Grb14	growth factor receptor bound protein 14	Yellow

APPENDIX 2 (CONTINUED): PROBE SETS DIFFERENTIALLY EXPRESSED BY NICKEL

Affymetrix ID	Gene Symbol	Gene Title	Cluster
1368674_at	Pygl	phosphorylase, glycogen, liver	Blue
1368835_at	Stat1	signal transducer and activator of transcription 1	Yellow
1368863_at	Nme3	non-metastatic cells 3, protein expressed in	Yellow
1368916_at	Asl	argininosuccinate lyase	Yellow
1369224_at	Cdh17	cadherin 17	Yellow
1369473_at	Pgm1	phosphoglucomutase 1	Blue
1369788_s_at	Jun	Jun oncogene	Blue
1369958_at	Rhob	ras homolog gene family, member B	Blue
1370030_at	Gclm	glutamate cysteine ligase, modifier subunit	Blue
1370062_at	Higd1a	HIG1 domain family, member 1A	Blue
1370120_at	Fstl3	follistatin-like 3 (secreted glycoprotein)	Blue
1370138_at	Lef1	lymphoid enhancer binding factor 1	Yellow
1370235_at	Dbi	diazepam binding inhibitor (GABA receptor modulator, acyl-Coenzyme A binding pro	Yellow
1370237_at	Hadh	hydroxyacyl-Coenzyme A dehydrogenase	Yellow
1370688_at	Gclc	glutamate-cysteine ligase, catalytic subunit	Blue
1370821_at	Tpmt	thiopurine S-methyltransferase	Yellow
1370848_at	Slc2a1	solute carrier family 2 (facilitated glucose transporter), member 1	Blue
1370954_at	P4ha1	procollagen-proline, 2-oxoglutarate 4-dioxygenase (proline 4-hydroxylase), alpha	Blue
1370959_at	Col3a1	collagen, type III, alpha 1	Yellow
1370975_at	Jmjd1a	jumonji domain containing 1A	Blue
1371005_at	Abcc1	ATP-binding cassette, sub-family C (CFTR/MRP), member 1	Blue
1371467_at	LOC293103	similar to RIKEN cDNA 0610007P06	Blue
1371824_at	Ak3l1	adenylate kinase 3-like 1	Blue
1372012_at	Dhcr24	24-dehydrocholesterol reductase	Yellow
1372178_at	---	---	Green
1372261_at	---	---	Blue
1372277_at	LOC641316	similar to aldehyde dehydrogenase 4 family, member A1	Yellow
1372318_at	---	---	Yellow

APPENDIX 2 (CONTINUED): PROBE SETS DIFFERENTIALLY EXPRESSED BY NICKEL

Affymetrix ID	Gene Symbol	Gene Title	Cluster
1372602_at	Stbd1	starch binding domain 1	Blue
1372610_at	P4ha2	procollagen-proline, 2-oxoglutarate 4-dioxygenase (proline 4-hydroxylase)	Blue
1372653_at	Fkbp11	FK506 binding protein 11	Blue
1372706_at	Hexb	hexosaminidase B	Blue
1372760_at	---	---	Blue
1372830_at	Arl6ip1	ADP-ribosylation factor-like 6 interacting protein 1	Blue
1372863_at	Mycbp2	MYC binding protein 2	Blue
1372993_at	---	---	Blue
1373026_at	Spc24	SPC24, NDC80 kinetochore complex component, homolog (S. cerevisiae)	White
1373036_at	RGD1561455	similar to Ras GTPase-activating-like protein IQGAP2	Yellow
1373037_at	Ube2l6	ubiquitin-conjugating enzyme E2L 6	Yellow
1373093_at	Errfi1	ERBB receptor feedback inhibitor 1	Blue
1373108_at	Ppp1r3c	protein phosphatase 1, regulatory (inhibitor) subunit 3C	Blue
1373433_at	Nsbp1	nucleosomal binding protein 1	Yellow
1373438_at	Ube2o	ubiquitin-conjugating enzyme E2O	Blue
1373475_at	Ccdc58	coiled-coil domain containing 58	Blue
1373524_at	---	---	Blue
1373544_at	Cxcl9	chemokine (C-X-C motif) ligand 9	Yellow
1373685_at	Ankrd37	ankyrin repeat domain 37	Blue
1373736_at	---	---	Blue
1373742_at	Spsb2	splA/ryanodine receptor domain and SOCS box containing 2	Yellow
1373807_at	Vegfa	vascular endothelial growth factor A	Blue
1373860_at	Sox4	SRY (sex determining region Y)-box 4	Blue
1373942_at	---	---	White
1374105_at	Higd1a	HIG1 domain family, member 1A	Blue
1374244_at	---	---	Yellow
1374433_at	---	---	Blue
1374447_at	Usp9x	ubiquitin specific peptidase 9, X-linked	Blue
1374524_at	Scly	selenocysteine lyase	Yellow

APPENDIX 2 (CONTINUED): PROBE SETS DIFFERENTIALLY EXPRESSED BY NICKEL

Affymetrix ID	Gene Symbol	Gene Title	Cluster
1374575_at	Creb3l1	cAMP responsive element binding protein 3-like 1	Yellow
1374632_at	Jmjd6	jumonji domain containing 6	Blue
1374663_at	---	---	Blue
1374778_at	Ctsc	cathepsin C	Yellow
1374828_at	Pdia5	protein disulfide isomerase family A, member 5	Blue
1374883_at	Mtmr7	myotubularin related protein 7	Yellow
1374906_at	Rnf113a1	ring finger protein 113A1	Blue
1374932_at	---	---	Blue
1374948_at	Tmem106a	transmembrane protein 106A	Blue
1375123_at	Sox4	SRY (sex determining region Y)-box 4	Blue
1375230_at	---	---	Blue
1375247_at	Mgll	Monoglyceride lipase	Yellow
1375362_at	Sppl2a	signal peptide peptidase-like 2A	Yellow
1375374_at	---	---	Green
1375388_at	---	---	Blue
1375532_at	---	---	Yellow
1375793_at	Mll1	myeloid/lymphoid or mixed-lineage leukemia 1	Blue
1375796_at	Igtp	interferon gamma induced GTPase	Yellow
1376151_a_at	---	---	Yellow
1376163_at	Clrn3	clarin 3	Yellow
1376677_a_at	---	---	Blue
1376724_at	---	---	Blue
1376917_at	Znf292	zinc finger protein 292	Blue
1377042_at	Pcgf5	polycomb group ring finger 5	Blue
1377043_at	---	---	Blue
1377234_at	---	---	Blue
1377277_at	---	---	Yellow
1377551_at	---	---	Blue
1377705_at	---	---	Blue
1377706_x_at	---	---	Blue
1377818_at	---	---	Blue

APPENDIX 2 (CONTINUED): PROBE SETS DIFFERENTIALLY EXPRESSED BY NICKEL

Affymetrix ID	Gene Symbol	Gene Title	Cluster
1377928_at	Tm4sf20	transmembrane 4 L six family member 20	Yellow
1378081_at	---	---	Blue
1378144_at	Kank4	KN motif and ankyrin repeat domains 4	Yellow
1378210_at	Mll1	myeloid/lymphoid or mixed-lineage leukemia 1	Blue
1378261_at	---	---	Blue
1378314_at	---	---	Blue
1378361_at	Chd7	chromodomain helicase DNA binding protein 7	Blue
1378413_at	---	---	Yellow
1378479_at	Cln3	ceroid-lipofuscinosis, neuronal 3	Yellow
1378808_at	---	---	Blue
1378833_at	---	---	Blue
1379356_at	---	---	Yellow
1379358_at	Samd4a	Sterile alpha motif domain containing 4A	Blue
1379365_at	Cxcl11	chemokine (C-X-C motif) ligand 11	Yellow
1379415_at	---	---	Blue
1379440_at	Fstl3	follistatin-like 3 (secreted glycoprotein)	Blue
1379452_at	Gas2	growth arrest-specific 2	Yellow
1379498_at	---	---	Blue
1379580_at	Chd6	chromodomain helicase DNA binding protein 6	Blue
1379636_at	Fam82a	family with sequence similarity 82, member A	Yellow
1379739_at	---	---	Blue
1379900_at	---	---	Yellow
1379932_at	Clcn4-2	chloride channel 4-2	Yellow
1379990_at	---	---	Blue
1380474_at	Loxl2	Lysyl oxidase-like 2	Blue
1380794_at	---	---	Blue
1380997_at	Ccnj	cyclin J	Blue
1381229_at	---	---	Blue
1381684_at	---	---	Blue
1381823_at	---	---	Blue
1381852_at	---	---	Yellow

APPENDIX 2 (CONTINUED): PROBE SETS DIFFERENTIALLY EXPRESSED BY NICKEL

Affymetrix ID	Gene Symbol	Gene Title	Cluster
1382001_at	LOC502710	similar to Myeloid/lymphoid or mixed-lineage leukemia protein 3 homolog	Blue
1382059_at	Fbxo30	F-box protein 30	Blue
1382072_at	Olfml2a	olfactomedin-like 2A	Yellow
1382255_at	---	---	Blue
1382266_at	Gpr146	G protein-coupled receptor 146	Blue
1382325_at	Gcat	glycine C-acetyltransferase (2-amino-3-ketobutyrate-coenzyme A ligase)	Yellow
1382348_at	Dhodh	dihydroorotate dehydrogenase	Blue
1382400_at	Rlf	rearranged L-myc fusion	Blue
1382658_at	LOC502710	similar to Myeloid/lymphoid or mixed-lineage leukemia protein 3 homolog (Histone	Blue
1382776_at	Mboat1	membrane bound O-acyltransferase domain containing 1	Yellow
1382797_at	RGD1560433	similar to 1500019C06Rik protein	Blue
1382924_at	Pank1	pantothenate kinase 1	Yellow
1382932_at	Lrrc50	leucine rich repeat containing 50	Blue
1382942_at	---	---	Blue
1382982_at	---	---	Blue
1383013_at	Klf13	Kruppel-like factor 13	Blue
1383058_at	---	---	Green
1383401_at	Tes	testis derived transcript	Blue
1383409_at	---	---	Blue
1383432_at	Dapl1	death associated protein-like 1	Yellow
1383500_at	Rrbp1	ribosome binding protein 1	Blue
1383785_at	Lef1	Lymphoid enhancer binding factor 1	Yellow
1383826_at	Rab40b	Rab40b, member RAS oncogene family	Blue
1383939_at	---	---	Blue
1384336_at	Cln3	ceroid-lipofuscinosis, neuronal 3	Yellow
1384406_at	LOC685243	similar to C-C chemokine receptor type 11 (C-C CKR-11) (CC-CKR-11) (CCR-11)	Yellow
1384432_at	---	---	Blue
1384475_at	---	---	Yellow
1384971_at	Depdc7	DEP domain containing 7	Yellow

APPENDIX 2 (CONTINUED): PROBE SETS DIFFERENTIALLY EXPRESSED BY NICKEL

Affymetrix ID	Gene Symbol	Gene Title	Cluster
1385050_at	Znf292	zinc finger protein 292	Blue
1385166_at	---	---	Yellow
1385171_s_at	Smtnl2	smoothelin-like 2	Blue
1385334_at	---	---	Yellow
1385706_at	---	---	Blue
1385827_at	Clcf1	cardiotrophin-like cytokine factor 1	Green
1386231_at	RGD1306474	similar to RIKEN cDNA 9530003J23	Yellow
1386352_at	---	---	Blue
1386695_at	---	---	Yellow
1386716_at	---	---	Yellow
1386773_at	Btd	biotinidase	Yellow
1386893_at	Grn	granulin	Yellow
1386908_at	Glrx1	glutaredoxin 1 (thioltransferase)	Yellow
1386946_at	Cpt1a	carnitine palmitoyltransferase 1a, liver	Yellow
1386958_at	Txnrd1	thioredoxin reductase 1	Blue
1386978_at	Bnip3l	BCL2/adenovirus E1B interacting protein 3-like	Blue
1387028_a_at	Id1	inhibitor of DNA binding 1	Blue
1387058_at	Pctp	phosphatidylcholine transfer protein	Yellow
1387060_at	Klf6	Kruppel-like factor 6	Green
1387121_a_at	Ndrg2	NDRG family member 2	Blue
1387130_at	Slc40a1	solute carrier family 39 (iron-regulated transporter), member 1	Blue
1387145_at	Gjb1	gap junction protein, beta 1	Yellow
1387178_a_at	Cbs	cystathionine beta synthase	Yellow
1387219_at	Adm	adrenomedullin	Blue
1387271_at	Phyh	phytanoyl-CoA 2-hydroxylase	Yellow
1387314_at	Sult1b1	sulfotransferase family, cytosolic, 1B, member 1	Yellow
1387338_s_at	Bcl2l11	BCL2-like 11 (apoptosis facilitator)	Blue
1387354_at	Stat1	signal transducer and activator of transcription 1	Yellow
1387361_s_at	Pgk1	phosphoglycerate kinase 1	Blue
1387528_at	Mbl2	mannose-binding lectin (protein C) 2	Yellow

APPENDIX 2 (CONTINUED): PROBE SETS DIFFERENTIALLY EXPRESSED BY NICKEL

Affymetrix ID	Gene Symbol	Gene Title	Cluster
1387805_at	Bnip3	BCL2/adenovirus E1B 19 kDa-interacting protein 3	Blue
1387893_at	C1s	complement component 1, s subcomponent	Yellow
1387914_at	Cyp27a1	cytochrome P450, family 27, subfamily a, polypeptide 1	Yellow
1387964_a_at	Ero1l	ERO1-like (S. cerevisiae)	Blue
1387995_a_at	Ifitm3	interferon induced transmembrane protein 3	Yellow
1388102_at	Ptgr1	prostaglandin reductase 1	Blue
1388108_at	Elovl6	ELOVL family member 6, elongation of long chain fatty acids (yeast)	Yellow
1388318_at	Pgk1	phosphoglycerate kinase 1	Blue
1388587_at	Ier3	immediate early response 3	Blue
1388600_at	---	---	Yellow
1388634_at	Pgm1	phosphoglucomutase 1	Blue
1388666_at	Enc1	ectodermal-neural cortex 1	Blue
1388742_at	---	---	Blue
1388872_at	---	---	Yellow
1388948_at	Stard10	StAR-related lipid transfer (START) domain containing 10	Yellow
1388985_at	---	---	Blue
1388986_at	---	---	Green
1389014_at	Nampt	nicotinamide phosphoribosyltransferase	Blue
1389075_at	---	---	Blue
1389132_at	Hip1	huntingtin interacting protein 1	Yellow
1389199_at	RGD1309079	similar to Ab2-095	Blue
1389207_at	Egln1	EGL nine homolog 1 (C. elegans)	Blue
1389230_at	---	---	Blue
1389297_at	Ero1l	ERO1-like (S. cerevisiae)	Blue
1389316_at	Usp9x	ubiquitin specific peptidase 9, X-linked	Blue
1389409_at	Tes	testis derived transcript	Blue
1389531_at	Zfp330	zinc finger protein 330	Green
1389555_at	Tcf19	transcription factor 19	White
1389618_at	---	---	Blue

APPENDIX 2 (CONTINUED): PROBE SETS DIFFERENTIALLY EXPRESSED BY NICKEL

Affymetrix ID	Gene Symbol	Gene Title	Cluster
1389797_at	---	---	Blue
1389858_at	Tk1	thymidine kinase 1, soluble	White
1390020_at	Ogdh	oxoglutarate (alpha-ketoglutarate) dehydrogenase (lipoamide)	Yellow
1390082_at	Hip1	huntingtin interacting protein 1	Yellow
1390109_at	---	---	Blue
1390203_at	---	---	Blue
1390394_at	LOC500034	similar to CG3570-PA	Blue
1390412_at	Slc40a1	solute carrier family 39 (iron-regulated transporter), member 1	Blue
1390423_at	Mycbp2	MYC binding protein 2	Blue
1390530_at	---	---	Yellow
1390532_at	---	---	Yellow
1390591_at	Slc17a3	solute carrier family 17 (sodium phosphate), member 3	Blue
1390709_at	Trio	triple functional domain (PTPRF interacting)	Blue
1390723_at	---	---	Blue
1390862_at	Znf629	zinc finger protein 629	Blue
1390932_at	---	---	Blue
1390945_at	Znf292	zinc finger protein 292	Blue
1390977_at	St7l	suppression of tumorigenicity 7-like	Blue
1390993_at	Pbld	phenazine biosynthesis-like protein domain containing	Yellow
1391212_at	Tceal1	transcription elongation factor A (SII)-like 1	Yellow
1391215_at	---	---	Blue
1391323_at	Srprb - Tf	signal recognition particle receptor, B subunit - transferrin	Blue
1391458_at	Ndrg1	N-myc downstream regulated gene 1	Blue
1391675_at	RGD1309708	similar to RIKEN cDNA 4930455F23	Blue
1391683_at	---	---	Blue
1391880_at	---	---	Blue
1392038_at	Arl6ip1	ADP-ribosylation factor-like 6 interacting protein 1	Blue

APPENDIX 2 (CONTINUED): PROBE SETS DIFFERENTIALLY EXPRESSED BY NICKEL

Affymetrix ID	Gene Symbol	Gene Title	Cluster
1392603_at	---	---	Blue
1392633_at	---	---	Blue
1392736_at	---	---	Blue
1392747_at	---	---	Blue
1392941_at	Hip1	huntingtin interacting protein 1	Yellow
1392946_at	---	---	Yellow
1392952_at	Acsf2	acyl-CoA synthetase family member 2	Yellow
1393047_at	Rnf217	ring finger protein 217	Blue
1393236_at	Riok3	RIO kinase 3 (yeast)	Blue
1393245_at	Phyh	Phytanoyl-CoA 2-hydroxylase	Yellow
1393377_at	---	---	Yellow
1393492_at	---	---	Blue
1393516_at	---	---	Yellow
1393612_a_at	Depdc7	DEP domain containing 7	Yellow
1393627_at	Osap	ovary-specific acidic protein	Blue
1394401_at	Elovl6	ELOVL family member 6, elongation of long chain fatty acids (yeast)	Yellow
1394459_at	FAM120C	family with sequence similarity 120C	Yellow
1394844_s_at	Cyp4a2 - Cyp4a3	cytochrome P450, family 4, subfamily a, polypeptide 2 - cytochrome P450, family	Yellow
1394948_at	---	---	Blue
1395041_at	Mttp	microsomal triglyceride transfer protein	Yellow
1395236_at	Ppp1r3c	protein phosphatase 1, regulatory (inhibitor) subunit 3C	Blue
1395427_at	---	---	White
1395519_at	MGC95152	similar to B230212L03Rik protein	Blue
1395744_at	---	---	Yellow
1395896_at	---	---	Blue
1396262_at	Nampt	nicotinamide phosphoribosyltransferase	Blue
1396539_at	---	---	Blue
1397304_at	Igtp	interferon gamma induced GTPase	Yellow
1397310_at	---	---	Blue
1397443_at	---	---	Blue
1397633_at	---	---	Green

APPENDIX 2 (CONTINUED): PROBE SETS DIFFERENTIALLY EXPRESSED BY NICKEL

Affymetrix ID	Gene Symbol	Gene Title	Cluster
1398380_at	Vwa1	von Willebrand factor A domain containing 1	Green
1398411_at	---	---	Blue
1398727_at	---	---	Yellow
1398791_at	Txnrd1	thioredoxin reductase 1	Blue
1398923_at	Rnasek	ribonuclease, RNase K	Yellow
1399119_at	Znf292	zinc finger protein 292	Blue
1397838_at	RGD1564792	RGD1564792	Blue
1374541_at	Gys1	glycogen synthase 1, muscle	Blue
1387671_at	Sctr	secretin receptor	Yellow
1389651_at	Apln	apelin	Blue
1391958_at	---	---	Blue
1372542_at	---	---	Blue
1372523_at	Gclc	glutamate-cysteine ligase, catalytic subunit	Blue
1374537_at	Chsy1	chondroitin sulfate synthase 1	Blue
1377902_a_at	Rad52	RAD52 homolog (S. cerevisiae)	Blue
1381902_at	Znf292	zinc finger protein 292	Blue
1385017_at	Aqr - Znf770	aquarius homolog (mouse) - zinc finger	Blue
1387622_at	Rfng	RFNG O-fucosylpeptide 3-beta-N-acetylglucosaminyltransferase	Yellow
1389641_at	Snapc4	small nuclear RNA activating complex, polypeptide 4	Blue
1392264_s_at	Serpine1	serine (or cysteine) peptidase inhibitor, clade E, member 1	Blue
1397709_at	Arl6ip1	ADP-ribosylation factor-like 6 interacting protein 1	Blue

APPENDIX 3: PROBE SETS DIFFERENTIALLY EXPRESSED BY CHROMIUM

Affymetix ID	Gene Symbol	Gene Title	Cluster
1367671_at	Pcna	proliferating cell nuclear antigen	White
1367790_at	Snd1	staphylococcal nuclease and tudor domain containing 1	Yellow
1367794_at	A2m	alpha-2-macroglobulin	Yellow
1367847_at	Nupr1	nuclear protein 1	Yellow
1367917_at	Cyp2d2	cytochrome P450, family 2, subfamily d, polypeptide 2	Yellow
1367983_at	Fen1	flap structure-specific endonuclease 1	White
1367994_at	Dpyd	dihydropyrimidine dehydrogenase	Yellow
1368060_at	Hrsp12	heat-responsive protein 12	Yellow
1368092_at	Fah	fumarylacetoacetate hydrolase	Yellow
1368204_at	Lig1	ligase I, DNA, ATP-dependent	White
1368224_at	Serpina3n	serine (or cysteine) peptidase inhibitor, clade A, member 3N	Yellow
1368244_at	As3mt	arsenic (+3 oxidation state) methyltransferase	Yellow
1368253_at	Gamt	guanidinoacetate N-methyltransferase	Yellow
1368387_at	Bdh1	3-hydroxybutyrate dehydrogenase, type 1	Yellow
1368399_a_at	Pgcp	plasma glutamate carboxypeptidase	Yellow
1368452_at	Abcc6	ATP-binding cassette, sub-family C (CFTR/MRP), member 6	Yellow
1368497_at	Abcc2	ATP-binding cassette, sub-family C (CFTR/MRP), member 2	Green
1368569_at	Akr1b7	aldo-keto reductase family 1, member B7	Yellow
1368642_at	Cdh2	cadherin 2	Yellow
1368658_at	Cntf	ciliary neurotrophic factor	White
1368707_at	Itih4	inter alpha-trypsin inhibitor, heavy chain 4	Yellow
1368860_at	Phlda1	pleckstrin homology-like domain, family A, member 1	Yellow
1368924_at	Ghr	growth hormone receptor	Yellow
1369086_a_at	Cacna1d	calcium channel, voltage-dependent, L type, alpha 1D subunit	Yellow
1369171_at	Mst1	Macrophage stimulating 1 (hepatocyte growth factor-like)	Yellow
1369225_at	Kng2	kininogen 2	Yellow
1369318_at	Fhit	fragile histidine triad gene	Yellow
1369610_at	Lin7c	lin-7 homolog C (C. elegans)	White
1369629_at	Adk	adenosine kinase	Yellow

APPENDIX 3 (CONTINUED): PROBE SETS DIFFERENTIALLY EXPRESSED BY CHROMIUM

Affymetix ID	Gene Symbol	Gene Title	Cluster
1369777_a_at	Shank2	SH3 and multiple ankyrin repeat domains 2	Yellow
1369837_at	Gulo	gulonolactone (L-) oxidase	Yellow
1369852_at	F10	coagulation factor X	Yellow
1369909_s_at	Tmem150	transmembrane protein 150	Yellow
1369940_at	Taldo1	transaldolase 1	White
1370127_at	Pold1	polymerase (DNA directed), delta 1, catalytic subunit	White
1370336_at	Osgin1	oxidative stress induced growth inhibitor 1	Blue
1370352_at	Cesl1 /// Es22 ///rCG_44273	carboxylesterase-like 1 /// esterase 22 ///carboxylesterase ES-4	White
1370436_at	Acsm2	acyl-CoA synthetase medium-chain family member 2	Yellow
1370475_at	Cyp2b3	cytochrome P450IIB3	Yellow
1370599_a_at	Ptprd	protein tyrosine phosphatase, receptor type, D	Yellow
1370615_at	LOC286989	UDP-glucuronosyltransferase	White
1370693_a_at	Cnp	2',3'-cyclic nucleotide 3' phosphodiesterase	Yellow
1370979_at	Ddx20	DEAD (Asp-Glu-Ala-Asp) box polypeptide 20	White
1370992_a_at	Fga	fibrinogen alpha chain	Yellow
1371014_at	Plcb1	phospholipase C, beta 1 (phosphoinositide-specific)	Yellow
1371069_at	Slc22a23	solute carrier family 22, member 23	Yellow
1371074_a_at	Mcm6	minichromosome maintenance complex component 6	White
1371081_at	Rapgef4	Rap guanine nucleotide exchange factor (GEF) 4	Yellow
1371094_at	Lhx2	LIM homeobox 2	White
1371099_at	---	---	Yellow
1371104_at	Srebf1	sterol regulatory element binding transcription factor 1	Yellow
1371124_a_at	Kng2	kininogen 2	Yellow
1371332_at	LOC684681	similar to Histone H1.2 (H1 VAR.1) (H1c)	Yellow
1371541_at	Mylk	myosin light chain kinase	Yellow
1371571_at	App	amyloid beta (A4) precursor protein	Yellow
1371572_at	App	amyloid beta (A4) precursor protein	Yellow
1371813_at	Hirip3	HIRA interacting protein 3	White

APPENDIX 3 (CONTINUED): PROBE SETS DIFFERENTIALLY EXPRESSED BY CHROMIUM

Affymetix ID	Gene Symbol	Gene Title	Cluster
1371942_at	Gstt3	glutathione S-transferase, theta 3	Yellow
1371963_at	Pcca	propionyl-coenzyme A carboxylase, alpha polypeptide	Yellow
1371970_at	Fam111a	family with sequence similarity 111, member A	White
1371988_at	Man1a1	mannosidase, alpha, class 1A, member 1	Yellow
1371990_at	Mpnd	MPN domain containing	Yellow
1371995_at	Klhl21	kelch-like 21 (Drosophila)	White
1372378_at	Dis3l2	DIS3 mitotic control homolog (S. cerevisiae)-like 2	Yellow
1372406_at	Mcm3	minichromosome maintenance complex component 3	White
1372438_at	Nit2	nitrilase family, member 2	Yellow
1372516_at	Kif22	kinesin family member 22	White
1372903_at	Kif18b	kinesin family member 18B	White
1373079_at	---	---	Yellow
1373178_at	---	---	Yellow
1373283_at	---	---	White
1373290_at	Ezh2	enhancer of zeste homolog 2 (Drosophila)	White
1373419_at	Ptprg	Protein tyrosine phosphatase, receptor type, G	Yellow
1373489_at	Chaf1a	chromatin assembly factor 1, subunit A (p150)	White
1373530_at	Ccne1	cyclin E1	White
1373557_at	Mcm4	minichromosome maintenance complex component 4	White
1373628_at	---	---	Yellow
1373654_at	Anxa8	annexin A8	Yellow
1373773_at	Gpm6a	glycoprotein m6a	Yellow
1373892_at	---	---	Yellow
1373908_at	---	---	Yellow
1373935_at	Pold2	polymerase (DNA directed), delta 2, regulatory subunit	White
1374036_at	Mcm2	minichromosome maintenance complex component 2	White
1374076_at	LOC690743 /// Rfwd3	similar to mixed lineage kinase domain-like /// ring finger and WD repeat domain	White

APPENDIX 3 (CONTINUED): PROBE SETS DIFFERENTIALLY EXPRESSED BY CHROMIUM

Affymetix ID	Gene Symbol	Gene Title	Cluster
1374222_at	Slc22a18	solute carrier family 22, member 18	Yellow
1374320_at	F5	coagulation factor V (proaccelerin, labile factor)	Yellow
1374359_at	Ccne2	cyclin E2	White
1374417_at	Nrbp2	nuclear receptor binding protein 2	Yellow
1374432_at	---	---	Yellow
1374495_at	Lrba	LPS-responsive vesicle trafficking, beach and anchor containing	Yellow
1374512_at	LOC684314	similar to CG9886-like	Yellow
1374532_at	Ptges2	prostaglandin E synthase 2	White
1374540_at	Cdca7	cell division cycle associated 7	White
1374747_at	Pftk1	PFTAIRE protein kinase 1	Yellow
1374861_at	Tle2	transducin-like enhancer of split 2 (E(sp1) homolog, Drosophila)	Yellow
1374911_at	RGD1303142	oxidative stress responsive gene	Green
1374915_at	---	---	Yellow
1374995_at	Elmo3	engulfment and cell motility 3	Yellow
1375026_at	Calml4	calmodulin-like 4	Yellow
1375224_at	Phlda3	pleckstrin homology-like domain, family A, member 3	White
1375314_at	Bcas3	breast carcinoma amplified sequence 3	Yellow
1375343_at	---	---	Yellow
1375517_at	Trp53inp2	tumor protein p53 inducible nuclear protein 2	Yellow
1375562_at	---	---	Yellow
1375612_at	---	---	Green
1375856_at	---	---	Yellow
1375857_at	Myof	myoferlin	Yellow
1375943_at	Cp110	CP110 protein	White
1376018_at	Lmnb2	Lamin B2	Green
1376026_at	Donson	downstream neighbor of SON	White
1376055_at	Mcm5	minichromosome maintenance complex component 5	White
1376071_at	---	---	Yellow
1376124_at	Iqub	IQ motif and ubiquitin domain containing	White
1376132_at	Gtdc1	glycosyltransferase-like domain containing 1	Yellow
1376317_at	Orc6l	origin recognition complex, subunit 6 like	White

APPENDIX 3 (CONTINUED): PROBE SETS DIFFERENTIALLY EXPRESSED BY CHROMIUM

Affymetix ID	Gene Symbol	Gene Title	Cluster
1376659_at	Nubpl	nucleotide binding protein-like	Yellow
1376687_at	Usp1	ubiquitin specific peptidase 1	White
1376731_at	---	---	Yellow
1376733_at	Igsf11	immunoglobulin superfamily, member 11	Yellow
1376747_at	---	---	Yellow
1376774_at	Exoc4	Exocyst complex component 4	Yellow
1376810_at	Mphosph8 /// Parp4	M-phase phosphoprotein 8 /// poly (ADP-ribose) polymerase family, member 4	Yellow
1376840_at	---	---	White
1376845_at	isg12(b)	putative ISG12(b) protein	Yellow
1376860_at	Slc22a23	solute carrier family 22, member 23	Yellow
1377114_at	---	---	Green
1377183_at	---	---	Yellow
1377254_a_at	Cohh1	Cohen syndrome homolog 1	Yellow
1377410_at	E2f8	E2F transcription factor 8	White
1377496_at	RGD1305441	similar to RIKEN cDNA 5730453I16	Green
1377718_at	Fancb	Fanconi anemia, complementation group B	White
1377832_at	Plk4	polo-like kinase 4 (Drosophila)	White
1377917_at	---	---	Green
1377962_at	Mybl2	myeloblastosis oncogene-like 2	White
1377967_at	Cdt1	chromatin licensing and DNA replication factor 1	White
1378056_at	Gmnn	geminin	White
1378334_a_at	---	---	Yellow
1378507_at	---	---	White
1378537_at	---	---	White
1378600_at	Taf1d	TATA box binding protein (TBP)-associated factor, RNA polymerase I, D, 41kDa	White
1378640_at	Uhrf1	ubiquitin-like with PHD and ring finger domains 1	White
1378766_at	---	---	Yellow
1378906_at	RGD1559690	similar to hypothetical protein FLJ25416	White
1379031_at	Gca	grancalcin	Yellow
1379073_at	Slc25a23	solute carrier family 25 (mitochondrial carrier; phosphate carrier), member 23	Yellow
1379076_at	---	---	Yellow

APPENDIX 3 (CONTINUED): PROBE SETS DIFFERENTIALLY EXPRESSED BY CHROMIUM

Affymetix ID	Gene Symbol	Gene Title	Cluster
1379393_at	Vil1	villin 1	Yellow
1379607_at	---	---	Yellow
1379608_at	RGD1560010	RGD1560010	White
1379673_at	Uap1l1	UDP-N-acteylglucosamine pyrophosphorylase 1-like 1	Yellow
1379696_at	---	---	Yellow
1379778_at	RGD1307983	similar to HSPC043 protein	White
1379815_at	LOC683733	similar to Transcription factor 7-like 2 (HMG box transcription factor 4) (T-cel	Yellow
1379904_at	Trappc6a	trafficking protein particle complex 6A	Yellow
1379957_at	Slfn8	schlafen 8	White
1379967_at	Zfp367	zinc finger protein 367	White
1379980_at	---	---	Yellow
1380013_at	Pnpla3	patatin-like phospholipase domain containing 3	Yellow
1380182_at	RGD1563437	similar to KIAA1217	Yellow
1380243_at	RGD1304693	similar to CG14803-PA	White
1380277_at	Rad51ap1	RAD51 associated protein 1	White
1380320_at	Lin54	lin-54 homolog (C. elegans)	White
1380598_at	---	---	Yellow
1380883_at	---	---	White
1381006_at	Hgfac	hepatocyte growth factor activator	Yellow
1381130_at	Mcm8	minichromosome maintenance complex component 8	White
1381574_at	Tmem195	transmembrane protein 195	Yellow
1381871_at	---	---	Yellow
1381982_at	Uap1l1	UDP-N-acteylglucosamine pyrophosphorylase 1-like 1	Yellow
1381983_at	Dennd1a	DENN/MADD domain containing 1A	Yellow
1382060_at	---	---	Yellow
1382218_at	RGD1305807	hypothetical LOC298077	Yellow
1382311_at	Tifa	TRAF-interacting protein with forkhead-associated domain	Yellow
1382431_at	---	---	Yellow
1382659_at	Pla2r1	phospholipase A2 receptor 1	Yellow
1382830_at	Suv39h2	suppressor of variegation 3-9 homolog 2 (Drosophila)	White

APPENDIX 3 (CONTINUED): PROBE SETS DIFFERENTIALLY EXPRESSED BY CHROMIUM

Affymetix ID	Gene Symbol	Gene Title	Cluster
1383103_at	Fam172a	family with sequence similarity 172, member A	Yellow
1383188_at	---	---	Yellow
1383212_at	---	---	Yellow
1383287_at	Fubp1	far upstream element (FUSE) binding protein 1	Green
1383458_at	---	---	Yellow
1383477_at	Uchl5	ubiquitin carboxyl-terminal hydrolase L5	Green
1383497_at	---	---	Yellow
1383574_at	Man1a1	mannosidase, alpha, class 1A, member 1	Yellow
1383604_at	---	---	Yellow
1383637_at	---	---	Yellow
1383640_at	---	---	Yellow
1383684_at	Asf1b	ASF1 anti-silencing function 1 homolog B (S. cerevisiae)	White
1383721_at	Fzd8	frizzled homolog 8 (Drosophila)	Green
1383728_at	LOC686240	similar to NMDA receptor regulated 1-like	Green
1383770_at	---	---	Yellow
1383853_at	Dyrk3	dual-specificity tyrosine-(Y)-phosphorylation regulated kinase 3	White
1383860_at	Fosl2	Fos-like antigen 2	White
1383900_at	Qrich2	glutamine rich 2	Yellow
1383921_at	---	---	White
1383931_at	---	---	Yellow
1383956_at	RGD1565709	similar to ovostatin-2	Yellow
1384041_at	---	---	White
1384068_at	Ckap2	cytoskeleton associated protein 2	White
1384103_at	RGD1561416	similar to novel protein (HT036)	Yellow
1384145_at	RGD1310495	similar to KIAA1919 protein	Yellow
1384231_at	LOC687121	similar to Shc SH2-domain binding protein 1	White
1384499_at	Bucs1	butyryl Coenzyme A synthetase 1	Yellow
1384701_at	---	---	White
1384818_at	Mylk	myosin light chain kinase	Yellow
1384988_at	Fbxo5	F-box protein 5	White
1385024_at	Cutc	cutC copper transporter homolog (E.coli)	Green
1385109_at	Taf1d	TATA box binding protein (TBP)-associated	White

APPENDIX 3 (CONTINUED): PROBE SETS DIFFERENTIALLY EXPRESSED BY CHROMIUM

Affymetix ID	Gene Symbol	Gene Title	Cluster
1385133_at	LOC691729	similar to spermatogenesis associated 5-like 1	White
1385381_at	---	---	Yellow
1385522_at	Orc1l	origin recognition complex, subunit 1-like (yeast)	White
1385733_at	Exo1	exonuclease 1	White
1385756_at	Itih1	inter-alpha trypsin inhibitor, heavy chain 1	Yellow
1385781_at	Ercc6l	excision repair cross-complementing rodent repair deficiency complementation gro	White
1386466_at	---	---	White
1387034_at	Pah	phenylalanine hydroxylase	Yellow
1387045_at	Atp6v0a1	ATPase, H+ transporting, lysosomal V0 subunit A1	Yellow
1387050_s_at	Kng1 /// Kng1l1 /// Kng2	kininogen 1 /// kininogen 1-like 1 /// kininogen 2	Yellow
1387307_at	Hal	histidine ammonia lyase	Yellow
1387411_at	Ptprk	protein tyrosine phosphatase, receptor type, K, extracellular region	Yellow
1387426_at	Slc25a21	solute carrier family 25 (mitochondrial oxodicarboxylate carrier), member 21	Yellow
1387457_at	Dusp12	dual specificity phosphatase 12	Green
1387530_a_at	Fosb /// Fosl2	FBJ osteosarcoma oncogene B /// fos-like antigen 2	White
1387599_a_at	Nqo1	NAD(P)H dehydrogenase, quinone 1	White
1387626_at	Dck	deoxycytidine kinase	White
1387673_a_at	Anxa6	annexin A6	Yellow
1387725_at	Gulo	gulonolactone (L-) oxidase	Yellow
1387795_at	Pola2	polymerase (DNA directed), alpha 2	White
1387872_at	Hnrnpa1	heterogeneous nuclear ribonucleoprotein A1	Green
1387907_at	Itpr1	inositol 1,4,5-triphosphate receptor, type 1	Yellow
1387924_at	Ngef	neuronal guanine nucleotide exchange factor	Yellow
1387963_a_at	Uox	urate oxidase	Yellow
1387972_at	Mucdhl	mucin and cadherin like	Yellow
1388135_at	Rpa2	replication protein A2	White
1388143_at	Col18a1	collagen, type XVIII, alpha 1	Yellow

APPENDIX 3 (CONTINUED): PROBE SETS DIFFERENTIALLY EXPRESSED BY CHROMIUM

Affymetix ID	Gene Symbol	Gene Title	Cluster
1388639_at	Bcas3	Breast carcinoma amplified sequence 3	Yellow
1388744_at	Mcm7	minichromosome maintenance deficient 7 (S. cerevisiae)	White
1388825_at	---	---	Yellow
1388870_at	Msi2	Musashi homolog 2 (Drosophila)	Yellow
1389102_at	Dock1	dedicator of cyto-kinesis 1	Yellow
1389136_at	Prkrir	protein-kinase, interferon-inducible double stranded RNA dependent inhibitor, re	White
1389150_at	---	---	Yellow
1389159_at	---	---	Yellow
1389248_at	Galk1	galactokinase 1	Yellow
1389371_at	---	---	Yellow
1389408_at	Rrm2	ribonucleotide reductase M2	White
1389421_at	Pole	polymerase (DNA directed), epsilon	White
1389434_at	Bbs9	Bardet-Biedl syndrome 9	Yellow
1389439_at	---	---	Green
1389440_at	---	---	White
1389448_at	4-Sep	septin 4	Yellow
1389457_at	Mybl2	myeloblastosis oncogene-like 2	White
1389510_at	Lyar	Ly1 antibody reactive homolog (mouse)	White
1389649_at	---	---	Yellow
1389725_at	Tm7sf2	transmembrane 7 superfamily member 2	Yellow
1389852_at	Cenpm	centromere protein M	White
1390389_at	---	---	Yellow
1390404_at	Lama2	laminin, alpha 2	Yellow
1390432_at	Tmco3	transmembrane and coiled-coil domains 3	Yellow
1390481_a_at	Ube2t	ubiquitin-conjugating enzyme E2T (putative)	White
1390557_at	Gca	grancalcin	Yellow
1390623_at	Gins3	GINS complex subunit 3 (Psf3 homolog)	White
1390650_at	Nup85	nucleoporin 85kDa	White
1390729_x_at	RGD1305441	similar to RIKEN cDNA 5730453I16	Green
1390823_at	Skp2	S-phase kinase-associated protein 2 (p45)	White
1390856_at	---	---	Yellow
1390982_at	Chaf1b	chromatin assembly factor 1, subunit B (p60)	White

APPENDIX 3 (CONTINUED): PROBE SETS DIFFERENTIALLY EXPRESSED BY CHROMIUM

Affymetix ID	Gene Symbol	Gene Title	Cluster
1391526_at	Kif16b	kinesin family member 16B	Yellow
1391538_at	Cideb	cell death-inducing DNA fragmentation factor, alpha subunit-like effector B	Yellow
1391544_at	---	---	Yellow
1391611_at	Kif12	kinesin family member 12	Yellow
1391621_at	---	---	Yellow
1391871_at	Stard13	StAR-related lipid transfer (START) domain containing 13	Yellow
1391890_at	Bcas3	breast carcinoma amplified sequence 3	Yellow
1391897_at	Rabgap1l	RAB GTPase activating protein 1-like	Yellow
1391916_at	---	---	Yellow
1392044_at	---	---	Yellow
1392057_at	LOC500893	similar to GLI-Kruppel family member GLI4	Blue
1392061_at	Mcm10	minichromosome maintenance complex component 10	White
1392064_at	Dlx1	distal-less homeobox 1	White
1392128_at	Atad5	ATPase family, AAA domain containing 5	White
1392440_at	---	---	White
1392554_a_at	---	---	White
1392653_at	---	---	Yellow
1392720_at	Cyp4f17	cytochrome P450, family 4, subfamily f, polypeptide 17	Yellow
1392800_at	RGD1308165	similar to hypothetical protein MGC17337	Blue
1392825_at	RGD1559600	RGD1559600	Yellow
1392852_at	Smoc1	SPARC related modular calcium binding 1	Yellow
1392870_at	---	---	Yellow
1393036_at	Psrc1	proline/serine-rich coiled-coil 1	White
1393123_at	C8g	complement component 8, gamma polypeptide	Yellow
1393228_at	Hpdl	4-hydroxyphenylpyruvate dioxygenase-like	White
1393230_s_at	RGD1308772	Similar to KIAA0564 protein	Yellow
1393260_at	LOC360228	WDNM1 homolog	Yellow
1393373_at	Opn3	opsin 3	White
1393561_at	---	---	Yellow
1393803_at	Casp8ap2	caspase 8 associated protein 2	White

APPENDIX 3 (CONTINUED): PROBE SETS DIFFERENTIALLY EXPRESSED BY CHROMIUM

Affymetix ID	Gene Symbol	Gene Title	Cluster
1393982_at	Pole2	polymerase (DNA directed), epsilon 2 (p59 subunit)	White
1394086_at	Senp7	SUMO1/sentrin specific protease 7	Yellow
1394371_at	Nufip1	nuclear fragile X mental retardation protein interacting protein 1	Blue
1394419_at	Arhgap11a	Rho GTPase activating protein 11A	White
1394457_at	---	---	White
1395132_at	Utrn	Utrophin	Yellow
1395203_at	---	---	Yellow
1395274_at	Dst	dystonin	Yellow
1395347_at	Arsa	arylsulfatase A	Yellow
1395644_at	Abca8	ATP-binding cassette, sub-family A (ABC1), member 8	Yellow
1395944_at	RGD1310778	similar to Putative protein C21orf45	White
1395957_at	---	---	Yellow
1396236_at	---	---	White
1396323_at	LOC681383	similar to Protein C10orf11 homolog	Yellow
1397286_at	---	---	Yellow
1397406_at	---	---	Yellow
1397409_s_at	Wee1	wee 1 homolog (S. pombe)	White
1397556_at	Nat13	N-acetyltransferase 13	Green
1397564_at	---	---	White
1397698_at	---	---	Yellow
1397704_at	LOC691979	similar to N-acetyltransferase ESCO2 (Establishment of cohesion 1 homolog 2)	White
1397915_at	---	---	White
1398397_at	---	---	Yellow
1398439_a_at	Orc6l	origin recognition complex, subunit 6 like (yeast)	White
1398546_at	---	---	White
1398598_at	Dst	dystonin	Yellow
1398706_at	---	---	White
1374131_at	---	---	Yellow
1369630_at	Adk	adenosine kinase	Yellow
1371862_at	Rrm1	ribonucleotide reductase M1	White
1376485_at	Traip	TRAF-interacting protein	White

APPENDIX 3 (CONTINUED): PROBE SETS DIFFERENTIALLY EXPRESSED BY CHROMIUM

Affymetix ID	Gene Symbol	Gene Title	Cluster
1383063_a_at	---	---	Yellow
1385132_at	---	---	White
1388526_at	Gstz1	glutathione transferase zeta 1	Yellow
1393848_at	Rrm2	ribonucleotide reductase M2	White
1374087_at	Slc48a1	solute carrier family 48 (heme transporter), member 1	White
1379277_at	---	---	Yellow
1383002_at	Phf20l1	PHD finger protein 20-like 1	Yellow
1387082_at	Fetub	fetuin B	Yellow
1387221_at	Gch1	GTP cyclohydrolase 1	Green
1391077_at	Clspn	claspin homolog (Xenopus laevis)	White
1393844_at	Mlf1ip	myeloid leukemia factor 1 interacting protein	White
1379386_at	Gtse1	G-2 and S-phase expressed 1	White

APPENDIX 4: PROBE SETS DIFFERENTIALLY EXPRESSED BY CADMIUM

Affymetrix ID	Gene Symbol	Gene Title	Cluster
1367631_at	Ctgf	connective tissue growth factor	Green
1367650_at	Tinagl1	tubulointerstitial nephritis antigen-like 1	Green
1367655_at	Tmsb10	thymosin, beta 10	Green
1367661_at	S100a6	S100 calcium binding protein A6	Green
1367729_at	Oat	ornithine aminotransferase (gyrate atrophy)	Yellow
1367764_at	Ccng1	cyclin G1	Green
1367784_a_at	Clu	clusterin	Green
1367800_at	Plat	plasminogen activator, tissue	Green
1367974_at	Anxa3	annexin A3	Green
1368072_at	Btg3	B-cell translocation gene 3	Green
1368162_at	Cst6	cystatin E/M	Green
1368167_at	Ctse	cathepsin E	Green
1368205_at	Cfi	complement factor I	Yellow
1368247_at	Hspa1a /// Hspa1b	heat shock 70kD protein 1A /// heat shock 70kD protein 1B (mapped)	Green
1368269_at	Lgals4	lectin, galactoside-binding, soluble, 4	Green
1368290_at	Cyr61	cysteine-rich, angiogenic inducer, 61	Green
1368332_at	Gbp2	guanylate binding protein 2	Green
1368335_at	Apoa1	apolipoprotein A-I	Green
1368339_at	S100g	S100 calcium binding protein G	Green
1368379_at	Scarb2	scavenger receptor class B, member 2	Green
1368380_at	Vtn	vitronectin	Yellow
1368490_at	Cd14	CD14 molecule	Green
1368538_at	Exoc7	exocyst complex component 7	Green
1368905_at	Ces2	carboxylesterase 2 (intestine, liver)	Green
1368947_at	Gadd45a	growth arrest and DNA-damage-inducible, alpha	Green
1369202_at	Mx2	myxovirus (influenza virus) resistance 2	Green
1369286_at	Proc	protein C	Yellow
1369590_a_at	Ddit3	DNA-damage inducible transcript 3	Green
1369701_at	Lipc	lipase, hepatic	Yellow
1370057_at	Csrp1	cysteine and glycine-rich protein 1	Green
1370073_at	Dnajc3	DnaJ (Hsp40) homolog, subfamily C, member 3	Green
1370153_at	Gdf15	growth differentiation factor 15	Green
1370174_at	Ppp1r15a	protein phosphatase 1, regulatory (inhibitor) subunit 15A	Green
1370223_at	Arfrp1	ADP-ribosylation factor related protein 1	Green

APPENDIX 4 (CONTINUED): PROBE SETS DIFFERENTIALLY EXPRESSED BY CADMIUM

Affymetrix ID	Gene Symbol	Gene Title	Cluster
1370259_a_at	Pthr1	parathyroid hormone receptor 1	Green
1370313_at	Acot7	acyl-CoA thioesterase 7	Green
1370348_at	Ninj1	ninjurin 1	Green
1370361_at	Cgref1	cell growth regulator with EF hand domain 1	Green
1370387_at	Cyp3a9	cytochrome P450, family 3, subfamily a, polypeptide 9	Green
1370399_at	Cyp4b1	cytochrome P450, family 4, subfamily b, polypeptide 1	Green
1370401_at	Ly6b	lymphocyte antigen 6 complex, locus B	Green
1370464_at	Abcb1	ATP-binding cassette, sub-family B (MDR/TAP), member 1	Green
1370583_s_at	Abcb1 /// Abcb1b	ATP-binding cassette, sub-family B (MDR/TAP), member 1 /// ATP-binding cassette,	Green
1370694_at	Trib3	tribbles homolog 3 (Drosophila)	Green
1370803_at	Zwint	ZW10 interactor	Green
1370912_at	Hspa1b	heat shock 70kD protein 1B (mapped)	Green
1370988_at	---	---	Green
1371015_at	Mx1	myxovirus (influenza virus) resistance 1	Green
1371211_a_at	Nrg1	neuregulin 1	Green
1371212_at	Nrg1	neuregulin 1	Green
1371455_at	Pmm1	phosphomannomutase 1	Green
1371689_at	---	---	Yellow
1371692_at	Mllt11	myeloid/lymphoid or mixed-lineage leukemia (trithorax homolog, Drosophila)	Green
1371703_at	Ahnak	AHNAK nucleoprotein	Green
1371735_at	---	---	Green
1371774_at	Sat1	spermidine/spermine N1-acetyl transferase 1	Green
1371785_at	Tnfrsf12a	tumor necrosis factor receptor superfamily, member 12a	Green
1372216_at	Cyb561d1	cytochrome b-561 domain containing 1	Green
1372240_at	Sgca	sarcoglycan, alpha (dystrophin-associated glycoprotein)	Green
1372306_at	Ethe1	ethylmalonic encephalopathy 1	Green
1372476_at	Fads3	fatty acid desaturase 3	Green
1372585_at	RGD1566254	RGD1566254	Green
1372604_at	RGD1309808	similar to apolipoprotein L2; apolipoprotein L-II	Green

APPENDIX 4 (CONTINUED): PROBE SETS DIFFERENTIALLY EXPRESSED BY CADMIUM

Affymetrix ID	Gene Symbol	Gene Title	Cluster
1372762_at	Hddc3	HD domain containing 3	Green
1388190_at	Apob	apolipoprotein B (including Ag(x) antigen)	Yellow
1388198_at	Nupl1	nucleoporin like 1	White
1372809_at	LOC290595	hypothetical gene supported by AF152002	Green
1372870_at	Kdelr3	KDEL (Lys-Asp-Glu-Leu) endoplasmic reticulum protein retention receptor 3	Green
1373490_at	Gmfg	glia maturation factor, gamma	Green
1373504_at	Glipr1	GLI pathogenesis-related 1	Green
1373606_at	Zfand2b	zinc finger, AN1 type domain 2B	Green
1374146_at	Mad2l2	MAD2 mitotic arrest deficient-like 2 (yeast)	Green
1374345_at	---	---	Green
1374610_at	---	---	Green
1375170_at	S100a11	S100 calcium binding protein A11 (calizzarin)	Green
1375346_at	RGD1563941	similar to hypothetical protein FLJ20010	Green
1375684_at	Neu1	sialidase 1 (lysosomal sialidase)	Green
1375906_at	LOC683034	hypothetical protein LOC683034	Green
1375920_at	Plekho1	pleckstrin homology domain containing, family O member 1	Green
1376319_at	Sema3c	sema domain, immunoglobulin domain (Ig), short basic domain, secreted	Green
1376500_at	Fbxo23	F-box only protein 23	Green
1377336_at	Sema3b	sema domain, immunoglobulin domain (Ig), short basic domain, secreted, (semaphor	Green
1377456_at	---	---	Yellow
1377739_at	Gng12	guanine nucleotide binding protein (G protein), gamma 12	Green
1377752_at	Emp2	epithelial membrane protein 2	Green
1378387_at	Tinf2	TERF1 (TRF1)-interacting nuclear factor 2	Green
1378570_at	---	---	Yellow
1378883_at	---	---	Yellow
1378896_at	Slc30a2	solute carrier family 30 (zinc transporter), member 2	Green
1378910_at	---	---	Green
1379318_at	LOC498662	similar to RIKEN cDNA 2610019F03	Green
1379420_at	RGD1565002	similar to Dehydrogenase/reductase SDR family member 7 precursor (Retinal short-	Yellow
1379805_at	Slc41a2	solute carrier family 41, member 2	Green

APPENDIX 4 (CONTINUED): PROBE SETS DIFFERENTIALLY EXPRESSED BY CADMIUM

Affymetrix ID	Gene Symbol	Gene Title	Cluster
1380470_x_at	---	---	Green
1380611_at	Fkbp5	FK506 binding protein 5	Green
1381082_at	RGD1564357	RGD1564357	Green
1381428_a_at	---	---	Yellow
1381453_at	---	---	Yellow
1381940_at	---	---	Green
1382028_at	Pex19	peroxisomal biogenesis factor 19	Yellow
1382137_at	Abhd3	abhydrolase domain containing 3	Green
1382475_at	---	---	Green
1382554_at	C8a	complement component 8, alpha polypeptide	Yellow
1382882_x_at	---	---	Green
1383248_at	Fmo5	flavin containing monooxygenase 5	Green
1383302_at	Dnajb1	DnaJ (Hsp40) homolog, subfamily B, member 1	Green
1383369_at	Trim26	tripartite motif-containing 26	Green
1383485_at	Mdm2	Mdm2 p53 binding protein homolog (mouse)	Green
1383666_at	Ptrh1	peptidyl-tRNA hydrolase 1 homolog (S. cerevisiae)	Green
1383702_at	---	---	Yellow
1383797_a_at	Ptrh1	peptidyl-tRNA hydrolase 1 homolog (S. cerevisiae)	Green
1383874_at	RGD1560812	RGD1560812	Green
1383999_at	---	---	Yellow
1384602_at	Gpr107	G protein-coupled receptor 107	Green
1385001_at	Gsdmd	gasdermin D	Green
1385089_at	Grhl1	grainyhead-like 1 (Drosophila)	Green
1385117_at	---	---	Green
1385252_at	Trim6	tripartite motif-containing 6	Green
1385269_s_at	Ccdc93	coiled-coil domain containing 93	Green
1385724_at	LOC682874	hypothetical protein LOC682874	Green
1385801_at	Dnajc18	DnaJ (Hsp40) homolog, subfamily C, member 18	Green
1385899_at	Trim16	tripartite motif-containing 16	Green
1386186_s_at	---	---	Green
1386879_at	Lgals3	lectin, galactoside-binding, soluble, 3	Green
1386890_at	S100a10	S100 calcium binding protein A10	Green
1386901_at	Cd36	CD36 molecule (thrombospondin receptor)	Yellow

APPENDIX 4 (CONTINUED): PROBE SETS DIFFERENTIALLY EXPRESSED BY CADMIUM

Affymetrix ID	Gene Symbol	Gene Title	Cluster
1387291_at	Itih3	inter-alpha trypsin inhibitor, heavy chain 3	Yellow
1387316_at	Cxcl1	chemokine (C-X-C motif) ligand 1 (melanoma growth stimulating activity, alpha)	Green
1387391_at	Cdkn1a	cyclin-dependent kinase inhibitor 1A (p21, Cip1)	Green
1387451_at	Dcbld2	discoidin, CUB and LCCL domain containing 2	Green
1387663_at	Gmfb	glia maturation factor, beta	Green
1387818_at	Casp4	caspase 4, apoptosis-related cysteine peptidase	Green
1387856_at	Cnn3	calponin 3, acidic	Green
1388130_at	Zyx	zyxin	Green
1388146_at	---	---	Yellow
1388453_at	Myadm	myeloid-associated differentiation marker	Green
1388460_at	Capg	capping protein (actin filament), gelsolin-like	Green
1388574_at	Wars	tryptophanyl-tRNA synthetase	Green
1388663_at	LOC687118	similar to death effector domain-containing DNA binding protein 2	Green
1388722_at	Dnajb1	DnaJ (Hsp40) homolog, subfamily B, member 1	Green
1388763_at	LOC690976	similar to Calponin-2 (Calponin H2, smooth muscle) (Neutral calponin)	Green
1388792_at	Gadd45g	growth arrest and DNA-damage-inducible, gamma	Green
1388924_at	Angptl4	angiopoietin-like 4	Green
1389068_at	Wipi2	WD repeat domain, phosphoinositide interacting 2	Green
1389110_at	---	---	Green
1389166_at	Cib2	calcium and integrin binding family member 2	Green
1389402_at	Axud1	AXIN1 up-regulated 1	Green
1389650_at	---	---	Yellow
1389732_at	Dram	damage-regulated autophagy modulator	Green
1389990_at	---	---	Green
1390026_at	Bag3	Bcl2-associated athanogene 3	Green
1390042_at	Tmem140	transmembrane protein 140	Yellow
1390391_at	---	---	Green

APPENDIX 4 (CONTINUED): PROBE SETS DIFFERENTIALLY EXPRESSED BY CADMIUM

Affymetrix ID	Gene Symbol	Gene Title	Cluster
1390691_at	RGD1561551	Similar to Hypothetical protein MGC75664	Green
1390770_at	---	---	Green
1391028_at	---	---	Green
1391571_at	---	---	Yellow
1392644_s_at	LOC498662	similar to RIKEN cDNA 2610019F03	Green
1393025_at	---	---	Green
1393134_at	Sephs1	selenophosphate synthetase 1	Yellow
1393584_at	Tnfrsf21	tumor necrosis factor receptor superfamily, member 21	Green
1394363_at	Riok3	RIO kinase 3 (yeast)	Green
1394923_at	LOC689619	similar to nuclear receptor interacting protein 2	Green
1395329_at	Gmppb	GDP-mannose pyrophosphorylase B	Green
1395366_at	---	---	Green
1395572_at	Dnaja4	DnaJ (Hsp40) homolog, subfamily A, member 4	Green
1395586_at	---	---	Yellow
1395699_at	Riok3	RIO kinase 3 (yeast)	Green
1396228_at	RGD1308958	Similar to chromosome 9 open reading frame 5	Green
1396383_at	Aldh3b1	aldehyde dehydrogenase 3 family, member B1	Green
1396561_x_at	Piga	phosphatidylinositol glycan anchor biosynthesis, class A	Green
1397372_at	Mobkl1b	MOB1, Mps One Binder kinase activator-like 1B (yeast)	Green
1398245_at	Sncg	synuclein, gamma (breast cancer-specific protein 1)	Green
1398264_at	Slc30a2	solute carrier family 30 (zinc transporter), member 2	Green
1398343_at	LOC498996	similar to DnaJ (Hsp40) homolog, subfamily A, member 4	Green
1398376_at	---	---	Green
1398600_at	---	---	Green
1398771_at	Slc3a2	solute carrier family 3 (activators of dibasic and neutral amino acid transport)	Green
1370244_at	Ctsl1	cathepsin L1	Green
1380668_at	MGC72974	Hypothetical LOC316976	Green
1387282_at	Hspb8	heat shock protein 8	Green

APPENDIX 4 (CONTINUED): PROBE SETS DIFFERENTIALLY EXPRESSED BY CADMIUM

1390662_at	Trim24	tripartite motif-containing 24	Green
1372729_at	Procr	protein C receptor, endothelial	Green
1379854_at	Abhd5	abhydrolase domain containing 5	Green
1387011_at	Lcn2	lipocalin 2	Green
1390455_at	Abhd2	abhydrolase domain containing 2	Green

APPENDIX 5: PROBE SETS DIFFERENTIALLY EXPRESSED BY NICKEL, CHROMIUM, AND CADMIUM

Affymetrix ID	Gene Symbol	Gene Title	Cluster
1367850_at	Fcgr2a -- LOC498276 -- LOC498277	Fc fragment of IgG, low affinity IIa, receptor (CD32) -- Fc gamma receptor II b	Green
1368342_at	Ampd3	adenosine monophosphate deaminase 3	Green
1368363_at	Klf5	Kruppel-like factor 5	Green
1368550_at	Foxq1	forkhead box Q1	Green
1369050_at	Pik3c2g	phosphoinositide-3-kinase, class 2, gamma polypeptide	Yellow
1369111_at	Fabp1	fatty acid binding protein 1, liver	Yellow
1369268_at	Atf3	activating transcription factor 3	Green
1370080_at	Hmox1	heme oxygenase (decycling) 1	Green
1370491_a_at	Hdc	histidine decarboxylase	Yellow
1370725_a_at	G6pc	glucose-6-phosphatase, catalytic subunit	Yellow
1371109_at	C8b	complement component 8, beta polypeptide	Yellow
1371237_a_at	Mt1a	metallothionein 1a	Green
1371527_at	Emp1	epithelial membrane protein 1	Green
1372727_at	---	---	Green
1373767_at	Zfand2a	zinc finger, AN1-type domain 2A	Green
1374886_at	Bcs1l	BCS1-like (yeast)	Blue
1380229_at	Maff	v-maf musculoaponeurotic fibrosarcoma oncogene homolog F (avian)	Blue
1380699_at	---	---	Green
1383253_at	---	---	Green
1383425_at	C5	complement component 5	Yellow
1383632_at	---	---	Green
1385961_at	Klf5	Kruppel-like factor 5	Green
1387228_at	Slc2a2	solute carrier family 2 (facilitated glucose transporter), member 2	Yellow
1388153_at	Acsl1	acyl-CoA synthetase long-chain family member 1	Yellow
1388271_at	Mt2A	metallothionein 2A	Green
1389381_at	Sqstm1	sequestosome 1	Green
1391806_at	LOC498793	similar to inter-alpha-inhibitor H2 chain	Yellow
1394039_at	Klf5	Kruppel-like factor 5	Green
1394112_at	Hao1	hydroxyacid oxidase 1	Yellow

APPENDIX 5 (CONTINUED): PROBE SETS DIFFERENTIALLY EXPRESSED BY NICKEL, CHROMIUM, AND CADMIUM

Affymetrix ID	Gene Symbol	Gene Title	Cluster
1398260_a_at	Serpind1	serine (or cysteine) peptidase inhibitor, clade D, member 1	Yellow
1398246_s_at	Fcgr2a LOC498276	Fc fragment of IgG, low affinity IIa, receptor (CD32) -- Fc gamma receptor II b	Green

APPENDIX 6: PROBE SETS DIFFERENTIALLY EXPRESSED BY NICKEL AND CADMIUM

Affymetrix ID	Gene Symbol	Gene Title	Cluster
1367584_at	Anxa2	annexin A2	Green
1367593_at	Sepw1	selenoprotein W, 1	Green
1367795_at	Ifrd1	interferon-related developmental regulator 1	Blue
1368146_at	Dusp1	dual specificity phosphatase 1	Green
1368147_at	Dusp1	dual specificity phosphatase 1	Green
1368940_at	P2ry2	purinergic receptor P2Y, G-protein coupled 2	Green
1369099_at	Slc30a1	solute carrier family 30 (zinc transporter), member 1	Green
1369736_at	Emp1	epithelial membrane protein 1	Green
1370000_at	Nucb2	nucleobindin 2	Blue
1370026_at	Cryab	crystallin, alpha B	Green
1370177_at	PVR	poliovirus receptor	Green
1371360_at	Ndrg1	N-myc downstream regulated gene 1	Blue
1372103_at	LOC498996	similar to DnaJ (Hsp40) homolog, subfamily A, member 4	Green
1372293_at	RGD1562059	Similar to RIKEN cDNA 1110038F21	Blue
1373677_at	Slc39a10	solute carrier family 39 (zinc transporter), member 10	Yellow
1374366_at	Slc39a4	solute carrier family 39 (zinc transporter), member 4	Yellow
1374404_at	Jun	Jun oncogene	Green
1376513_a_at	---	---	Green
1377626_at	LOC690768	hypothetical protein LOC690768	Yellow
1379934_at	---	---	Blue
1381335_at	---	---	Green
1381533_at	Rnd1	Rho family GTPase 1	Green
1383193_at	---	---	Green
1383744_at	---	---	Green
1385464_at	Foxq1	Forkhead box Q1	Green
1386944_a_at	G6pc	glucose-6-phosphatase, catalytic subunit	Yellow
1388267_a_at	Mt1a	metallothionein 1a	Green
1388721_at	Hspb8	heat shock protein 8	Green
1388900_at	RGD1566118	RGD1566118	Green
1389528_s_at	Jun	Jun oncogene	Green

APPENDIX 6 (CONTINUED): PROBE SETS DIFFERENTIALLY EXPRESSED BY NICKEL AND CADMIUM

Affymetrix ID	Gene Symbol	Gene Title	Cluster
1391481_at	---	---	Green
1392579_at	Obfc2a	oligonucleotide/oligosaccharide-binding fold containing 2A	Green
1392627_x_at	---	---	Green
1398296_at	Gde1	glycerophosphodiester phosphodiesterase 1	Blue
1390287_at	Bin2 -- LOC685015	bridging integrator 2 -- hypothetical protein LOC685015	Yellow

APPENDIX 7: PROBE SETS DIFFERENTIALLY EXPRESSED BY NICKEL AND CHROMIUM

Affymetrix ID	Gene Symbol	Gene Title	Cluster
1367598_at	Ttr	transthyretin	Yellow
1367909_at	Dcxr	dicarbonyl L-xylulose reductase	Yellow
1368180_s_at	Gsta2 /// LOC494499	glutathione S-transferase A2 /// LOC494499 protein	Blue
1368278_at	Lgals2	lectin, galactoside-binding, soluble 2	Yellow
1368627_at	Rgn	regucalcin (senescence marker protein-30)	Yellow
1369499_at	Tyms	thymidylate synthetase	White
1370019_at	Sult1a1	sulfotransferase family, cytosolic, 1A, phenol-preferring, member 1	Yellow
1370264_at	Syne1	spectrin repeat containing, nuclear envelope 1	Yellow
1370310_at	Hmgcs2	3-hydroxy-3-methylglutaryl-Coenzyme A synthase 2 (mitochondrial)	Yellow
1370902_at	Akr1b8	aldo-keto reductase family 1, member B8	Blue
1370939_at	Acsl1	acyl-CoA synthetase long-chain family member 1	Yellow
1372006_at	---	---	Blue
1372101_at	Ppap2b	phosphatidic acid phosphatase type 2B	Yellow
1372398_at	Kctd15	potassium channel tetramerisation domain containing 15	Blue
1373035_at	---	---	Blue
1374615_at	---	---	Yellow
1374758_at	---	---	Yellow
1376640_at	Fam171a1	Family with sequence similarity 171, member A1	Yellow
1377758_at	Hsd17b13	hydroxysteroid (17-beta) dehydrogenase 13	Yellow
1377878_at	Fgfbp3	fibroblast growth factor binding protein 3	Green
1378133_at	Slc7a11	solute carrier family 7 (cationic amino acid transporter, y+ system), member 11	Blue
1379240_at	---	---	Yellow
1380610_at	---	---	Blue
1380682_at	Mex3b	mex3 homolog B (C. elegans)	Blue
1383472_at	Aldh1b1	aldehyde dehydrogenase 1 family, member B1	Yellow
1383578_at	Rad51	RAD51 homolog (RecA homolog, E. coli) (S. cerevisiae)	White
1383603_at	---	---	Yellow
1384505_at	---	---	Yellow
1385569_at	---	---	Blue

APPENDIX 7 (CONTINUED): PROBE SETS DIFFERENTIALLY EXPRESSED BY NICKEL AND CHROMIUM

Affymetrix ID	Gene Symbol	Gene Title	Cluster
1387808_at	Slc7a7	solute carrier family 7 (cationic amino acid transporter, y+ system), member 7	Yellow
1387809_at	Map2k6	mitogen-activated protein kinase kinase 6	Yellow
1388340_at	Ns5atp9	NS5A (hepatitis C virus) transactivated protein 9	White
1389054_at	LOC498368	similar to RIKEN cDNA 0610040J01	Yellow
1389265_at	Gbe1	glucan (1,4-alpha-), branching enzyme 1	Blue
1389662_at	Wnk4	WNK lysine deficient protein kinase 4	Yellow
1390024_at	---	---	Yellow
1390715_at	Igfbpl1	insulin-like growth factor binding protein-like 1	Yellow
1391450_at	Loxl2	lysyl oxidase-like 2	Blue
1392037_at	---	---	Yellow
1392384_s_at	Akr1d1	aldo-keto reductase family 1, member D1 (delta 4-3-ketosteroid-5-beta-reductase)	Yellow
1393119_at	---	---	Green
1393615_at	Depdc6	DEP domain containing 6	Yellow
1396189_at	---	---	Blue
1396190_x_at	---	---	Blue
1398620_at	Samd4a	Sterile alpha motif domain containing 4A	Blue
1398634_at	LOC686032	hypothetical protein LOC686032	Yellow
1387234_at	Azgp1	alpha-2-glycoprotein 1, zinc-binding	Yellow

APPENDIX 8: PROBE SETS DIFFERENTIALLY EXPRESSED BY CHROMIUM AND CADMIUM

Affymetrix ID	Gene Symbol	Gene Title	Cluster
1367647_at	Serpina1	serpin peptidase inhibitor, clade A (alpha-1 antiproteinase, antitrypsin), membe	Yellow
1367988_at	Cyp2c23	cytochrome P450, family 2, subfamily c, polypeptide 23	Yellow
1368064_a_at	Ddc	dopa decarboxylase (aromatic L-amino acid decarboxylase)	Yellow
1368360_at	Plg	plasminogen	Yellow
1368741_at	C9	complement component 9	Yellow
1368806_at	Sepp1	selenoprotein P, plasma, 1	Yellow
1369455_at	Abcg5	ATP-binding cassette, sub-family G (WHITE), member 5	Yellow
1369790_at	Tat	tyrosine aminotransferase	Yellow
1369840_at	UST4r	integral membrane transport protein UST4r	Yellow
1370027_a_at	LOC297568 -- Mug1	alpha-1-inhibitor III -- murinoglobulin 1	Yellow
1370151_at	Cps1	carbamoyl-phosphate synthetase 1, mitochondrial	Yellow
1370299_at	Aldob	aldolase B, fructose-bisphosphate	Yellow
1370547_at	Pzp	pregnancy-zone protein	Yellow
1372805_at	RGD1310444	LOC363015	Green
1373718_at	Tubb2a	tubulin, beta 2a	Green
1373803_a_at	Ghr	growth hormone receptor	Yellow
1374139_at	Cdr2	cerebellar degeneration-related 2	Green
1374650_at	Nedd9	neural precursor cell expressed, developmentally down-regulated 9	Yellow
1375633_at	Clic1	chloride intracellular channel 1	Green
1376098_a_at	Myo1g	myosin IG	Green
1377222_at	---	---	Yellow
1377461_at	LOC680485	hypothetical protein LOC680485	Green
1379324_at	---	---	Yellow
1379376_at	---	---	Green
1382358_at	---	---	Yellow
1383046_at	Cfh	complement factor H	Yellow
1383164_at	---	---	Yellow
1383169_at	---	---	Yellow

APPENDIX 8 (CONTINUED): PROBE SETS DIFFERENTIALLY EXPRESSED BY CHROMIUM AND CADMIUM

Affymetrix ID	Gene Symbol	Gene Title	Cluster
1385043_at	Inadl	InaD-like (Drosophila)	Yellow
1387508_at	Baat	bile acid Coenzyme A: amino acid N-acyltransferase (glycine N-choloyltransferase	Yellow
1388229_a_at	Mug1	murinoglobulin 1	Yellow
1388459_at	Col18a1	collagen, type XVIII, alpha 1	Yellow
1389913_at	Lrrfip1	leucine rich repeat (in FLII) interacting protein 1	Green
1396053_at	Nedd9	neural precursor cell expressed, developmentally down-regulated 9	Yellow
1384544_at	Pon3	paraoxonase 3	Yellow
1384427_at	Mdm2	Mdm2 p53 binding protein homolog (mouse)	Green